Aquaculture 559 (2022) 738430

Contents lists available at ScienceDirect

Aquaculture

journal homepage: www.elsevier.com/locate/aquaculture

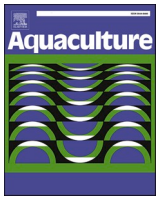

What will happen to my smolt at harvest? Individually tagged Atlantic salmon help to understand possible progression and regression of vertebral deformities

Lucia Drábiková [a,*], Per Gunnar Fjelldal [b], Adelbert De Clercq [c,d], M. Naveed Yousaf [e], Thea Morken [e], Charles McGurk [e], P. Eckhard Witten [a,*]

[a] Evolutionary Developmental Biology, Biology Department, Ghent University, Ledeganckstraat 35, 9000 Ghent, Belgium
[b] Institute of Marine Research (IMR), Matre Research Station, N-5984 Matredal, Norway
[c] Center for Medical Genetics Ghent, Biomolecular Medicine Department, Ghent University, Corneel Heymanslaan 10, 9000 Ghent, Belgium
[d] Flanders Research Institute for Agriculture, Fisheries and Food (ILVO), Ankerstraat 1, 8400 Oostende, Belgium
[e] Skretting Aquaculture Innovation, P.O. Box 48, N-4001 Stavanger, Norway

ARTICLE INFO

Keywords:
Atlantic salmon
Deformity development
Intervertebral joint
Hyper-dense vertebrae
Recovery

ABSTRACT

Vertebral deformities can impair health, welfare, and product quality in farmed Atlantic salmon. Deformities detected early in the production cycle raise questions about their further development: which types of deformities will progress and which types of deformities will worsen over time? To study this, Atlantic salmon parr (start experimental feeding weight 13.5 g) were fed diets with low (6.8 g/kg), regular (10.0 g/kg), or high (13.0 g/kg) total dietary P for 11 weeks to provoke deformities. This was followed by long-term monitoring of deformity development up to harvest size (4.5 kg) through repeated radiology of individually tagged animals. Further insights were obtained by histological analyses, mineral analyses, and testing for mechanical properties of vertebral centra. Four categories of deformity development were defined: (1) recovery, (2) containment, (3) progression, and (4) late-onset. Deformities detected early, in freshwater, which affected the vertebral centra but not the intervertebral joints, could fully recover in seawater. These involved low-mineralised vertebrae, single vertically shifted vertebrae, hyper-dense vertebrae (HDV), and two or three adjacent vertebrae with compression-related deformities. HDV were provoked by low dietary P but disappeared in seawater. Fusions were either contained (two to three vertebrae) (stable vertebral fusions) or progressed (more than three vertebrae) (progressive vertebral fusions). Vertical shifts, fusions, and compressions could also have a late-onset in seawater but did not develop into severe deformities in harvest size animals. In conclusion, low-mineralised vertebrae and HDV are abundant in animals with LP diet history but can recover in seawater. The frequency of all other types of deformities was not significantly different among animals of different diet history groups. Under the current experimental conditions, a period of high or low dietary P in freshwater had no significant effect on the prevalence of early- or late-onset deformities at harvest.

1. Introduction

Vertebral deformities are observed in both wild and farmed Atlantic salmon (*Salmo salar* L.) (Fjelldal et al., 2012; Kvellestad et al., 2000; Madaro et al., 2021; Sambraus et al., 2014; Witten et al., 2005). Severe vertebral deformities can result in growth retardation and have a negative impact on the animals' health and welfare (Hansen et al., 2010; Kvellestad et al., 2000; Witten et al., 2006). Eventually, deformities may also lead to product quality degradation (Fjelldal et al., 2012; Fraser et al., 2019; Kvellestad et al., 2000; Munday et al., 2016). Early life stages are particularly sensitive to increased temperatures or heat shock and can develop severe deformities of the notochord. Typical deformities that relate to early developmental defects observed in first feeding animals and in later stages are compression and fusion of vertebral centra anlagen (De Clercq et al., 2017a; Wargelius et al., 2005; Ytteborg et al., 2010a). The development of similar deformities has also been reported to start in later Atlantic salmon freshwater stages (Fjelldal et al., 2007a; Grini et al., 2011; Smedley et al., 2018). Deformities also

* Corresponding authors.
E-mail addresses: lucia.drabikova@ugent.be (L. Drábiková), peckhardwitten@aol.com (P.E. Witten).

https://doi.org/10.1016/j.aquaculture.2022.738430
Received 3 February 2022; Received in revised form 24 May 2022; Accepted 27 May 2022
Available online 30 May 2022
0044-8486/© 2022 The Authors. Published by Elsevier B.V. This is an open access article under the CC BY-NC-ND license (http://creativecommons.org/licenses/by-nc-nd/4.0/).

affect differentiated, but still growing, vertebral centra. Water quality, temperature, and dietary mineral supply are considered as important parameters for healthy skeletal development in salmonids (Clarkson et al., 2021; De Clercq et al., 2017a; Grini et al., 2011; Lall, 2022; Sánchez et al., 2011; Wargelius et al., 2005; Ytteborg et al., 2010a, 2010b). Vertebral column deformities can also be caused by high water current velocity, typically lordosis in the caudal region of the vertebral column in European sea bass (*Dicentrarchus labrax*), Gilthead sea bream (*Sparus aurata*), and zebrafish (*Danio rerio*). In the literature this deformity type is also designated as haemal lordosis (Fragkoulis et al., 2019, 2022; Printzi et al., 2021).

Dietary mineral supply is linked to the development of bone and is thus an important factor for skeletal health (Lall and Lewis-McCrea, 2007). The critical dietary mineral for skeletal mineralisation in teleosts is phosphorous (P) (Witten and Huysseune, 2009). Skeletal elements of the endoskeleton (jaws and vertebral bodies) and dermal skeleton (opercula and scales) show equal reduction of the mineral content in response to low dietary P intake in Atlantic salmon (Drábiková et al., 2021; Helland et al., 2005; Witten et al., 2016). Dietary P deficiency in Atlantic salmon has also been linked to vertebral deformities such as reduced intervertebral spaces, homogenous compression, and hyperdense vertebrae (HDV) (Fjelldal et al., 2016; Helland et al., 2006; Smedley et al., 2018; Ytteborg et al., 2016). Although increased dietary P levels have been suggested to prevent vertebral deformities (Baeverfjord et al., 2019; Fjelldal et al., 2009a, 2012), other studies show no further positive effects of high dietary P on skeletal health or growth rate in Atlantic salmon (Drábiková et al., 2021; Witten et al., 2016, 2019). Furthermore, Atlantic salmon can handle periods of P deficiency without developing vertebral deformities (Drábiková et al., 2021; Witten et al., 2016, 2019).

Early detection is of key importance to a proper management of deformities in Atlantic salmon (Sullivan et al., 2007). Deformities that are detected early, *i.e.* prior to seawater transfer, raise questions about the progression of specific deformity types. Particularly, which types of deformities can have a negative impact on animal welfare and eventually reduce the product quality? There are 20 types of vertebral deformities recognised in Atlantic salmon (Witten et al., 2009). These are grouped into four categories: (i) compressed and fused vertebral bodies, (ii) radiolucent and radiopaque vertebral bodies, (iii) spine curvatures, symmetry deviations, and displacement of vertebral bodies, and (iv) severe multiple malformations (Witten et al., 2009). Common types of deformities in Atlantic salmon are associated with compression and fusion (Fjelldal et al., 2012; Witten et al., 2005, 2006). Previous studies have shown that not all types of deformities constitute a problem for animal welfare (Hansen et al., 2010; Sambraus et al., 2014). Moreover, several deformities also occur in wild Atlantic salmon (Sambraus et al., 2014). In addition, Atlantic salmon has the capacity to contain a fusion of up to three consecutive vertebrae through the reshaping and remodelling of the fused vertebrae into a single, and eventually regularly structured, vertebral centrum (Witten et al., 2006; Sambraus et al., 2014). Such a stable vertebral fusion is only recognisable by the presence of two or three neural and haemal arches or ribs and is not associated with ectopic fibrous connective tissue in the muscle. The failure to contain vertebral fusion leads to the development of large progressive vertebral fusion (Witten et al., 2006). Progressive vertebral fusion and several consecutive homogenously compressed or cross-stitched vertebrae are severe deformities from which ectopic fibrous connective tissues can extend into the muscles (Fraser et al., 2019; Holm et al., 2020; Kvellestad et al., 2000; Sullivan et al., 2007; Vågsholm and Djupvik, 1998). So far, a few studies analysed vertebral deformities in individually tagged Atlantic salmon (Fjelldal et al., 2007b; Witten et al., 2006), Atlantic cod (*Gadus morhua*) (Fjelldal et al., 2009b), Chinook salmon (*Oncorhynchus tshawytscha*) (Walbaum, 1792) (Lovett et al., 2020), European seabass (Fragkoulis et al., 2022), and Gilthead seabream (Fragkoulis et al., 2019). Long-term studies in Atlantic salmon indicate that the future development of a progressive vertebral fusion can be recognised already in the freshwater phase, however other deformities (dislocation and homogenous compression) can develop *de novo* later in the seawater phase of Atlantic salmon (Fjelldal et al., 2007b; Witten et al., 2006). Further knowledge is required to postulate the fate of deformities that are diagnosed in freshwater. This may allow a better prediction of bone health and improve animal welfare.

This study aims to answer two questions about the progression of vertebral deformities in Atlantic salmon. First, what are the long-term consequences of low, regular, and high dietary P intake during the animals' sensitive freshwater phase? Second, which types of deformities detected prior to seawater transfer and later in seawater develop into severe deformities and constitute a risk for the animals' welfare and product quality at harvest? To answer these questions, Atlantic salmon parr were fed for 11 weeks (week 2–13) with low P, regular P, and high P diets, were individually PIT-tagged, and x-rayed at week 15 (prior to seawater transfer), 47, and 84 when animals reached harvest size.

2. Materials and methods

2.1. Fish stock

The study was performed in agreement with Norwegian legislation and approved by the Norwegian Food Safety Authority (FOTS ID 19123). The trial was carried out at Skretting Aquaculture Innovation Lerang Research Station (Forsand, Norway) using the Atlantic salmon strain from Benchmark Genetics (Iceland). Eggs were fertilised in July 2018 and transported to Lerang Research Station at eyed egg stage. The eggs were incubated at 8 °C. Animals hatched in September and were reared at 8 °C. From start-feeding, animals were kept in indoor tanks of 2000 *l* at a temperature of 12 °C, under 24 h light regime, and a maximum density of 51.3 kg/m^3. In January, animals were moved to outdoor tanks with a volume of 30,000 *l*. The water temperature was measured once a week and ranged from 3 °C in January to 7.5 °C in mid-February. The maximum density was 27.1 kg/m^3.

2.1.1. Freshwater trial

Animals were transferred to nine 70 *l* tanks (Fig. 1) at a density of 14.3 kg/m^3 and a temperature of 10.4 °C. Animals were acclimatised for two weeks at 12 °C (Fig. 1). The photoperiod was set to 12 h of light and 12 h of dark. Animals were fed a commercial diet, Nutra Olympic, pellet size 1.5 mm (Skretting, Norway) during the acclimatisation period. At week 2, all animals were anaesthetised with MS-222 (Tricaine methanesulphonate, Pharmaq, Norway), graded, and 36 animals were sampled (see analysis Fig. 1). At the start of the P feeding trial animals were returned to their respective tanks at a density of 9.5 kg/m^3 (Fig. 1). Animals were left undisturbed throughout the 11-week long P feeding trial without mechanical stress associated with handling, grading, and vaccination.

During the P feeding trial animals were maintained under 12 h of light and 12 h of dark photoperiod to prevent premature onset of smoltification (Björnsson et al., 2000). Salinity (0.29 ± 0.12 ppt), oxygen levels (94.23 ± 6.84%), and temperature (12.40 ± 0.13 °C) were monitored daily. The maximum density at the end of the P feeding trial was 19.9 kg/m^3. Direction of swimming within the tanks was anticlockwise against the water current. Three isocaloric and iso-nitrogenous pre-smolt diets were formulated to different dietary total P (see Table 1 in Drábiková et al., 2021), extruded as 2 mm pellets at Skretting Aquaculture Innovation Feed Technology Plant (Stavanger, Norway) and provided to the animals continuously using automatic feeders (Hølland Teknologi AS, Sandnes, Norway). Animals were fed for 14 s with 161 s intervals between feeding events irrespective of the photoperiod. Three diets contained different levels of total P (tP) and soluble P (sP), respectively: low P (LP) = 6.8 g/kg tP, 3.5 g/kg sP, regular P (RP) = 10.0 g/kg tP, 5.6 g/kg sP, and high P (HP) = 13.0 g/kg tP, 9.3 g/kg *sP*. Dietary P levels were met by adjusting the supplementation of inorganic P in the form of mono-ammonium phosphate (see Table 1 in

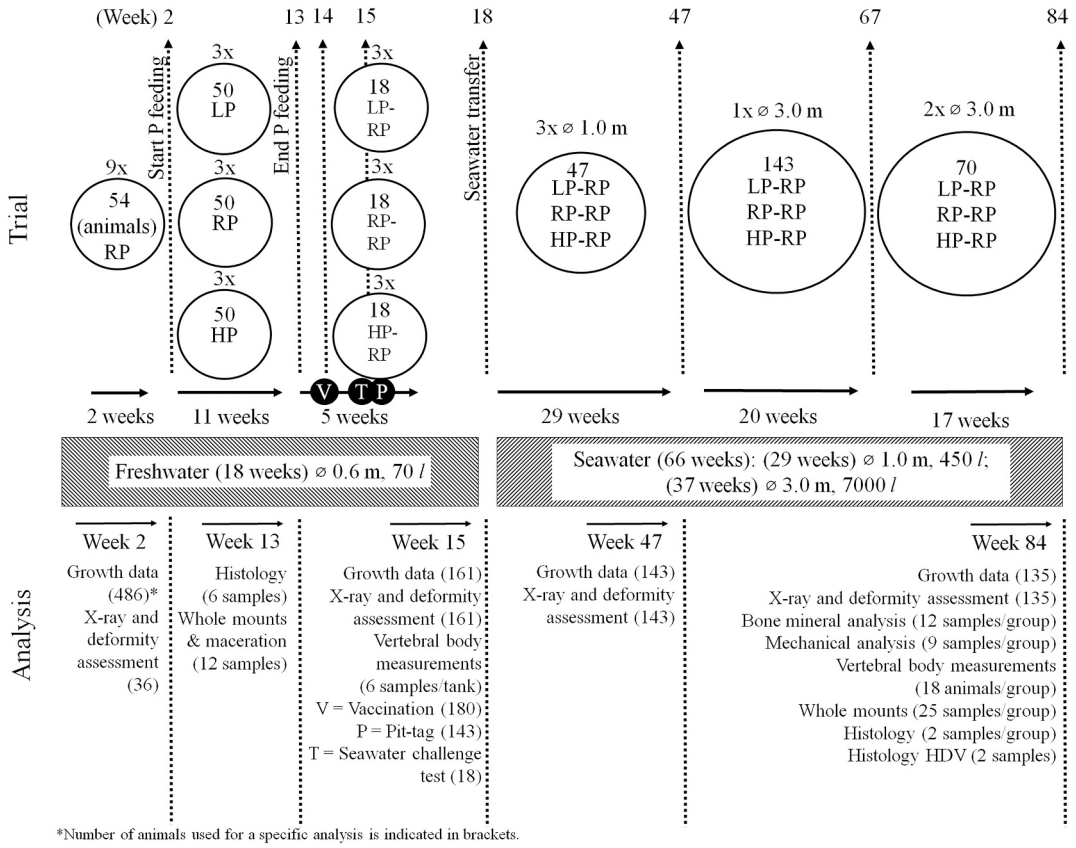

Fig. 1. Experimental set-up and analysis. Animals were reared in freshwater for 18 weeks in nine tanks (V = 70 *l*, ⌀ = 0.6 m). Animals were acclimatised for two weeks prior to phosphorus (P) feeding. Atlantic salmon were subsequently fed diets with low (LP), regular (RP), or high dietary P (HP) for 11 weeks (week 2–13) in freshwater. Thereafter all animals were fed commercial diets with RP. All animals were vaccinated (V) at week 14. Animals were PIT-tagged (P) at week 15. Two animals per tank were subjected to a seawater challenge test (T). At week 18, animals were transferred to three seawater tanks (V = 450 *l*, ⌀ = 1.0 m) each tank containing animals from all three diet groups. At week 47, animals were transferred to a larger tank (V = 7000 *l*, ⌀ = 3.0 m) and at week 67, animals were further split into two tanks (V = 7000 *l*, ⌀ = 3.0 m). The trial was terminated at week 84. Analyses and types of samples taken at specified time-points are indicated.

Drábiková et al., 2021).

2.1.2. Seawater transfer and a follow-up trial

After the P feeding trial, animals were vaccinated (Alpha Ject micro 6, Pharmaq, Norway) at week 14 (V in Fig. 1). Two animals per tank were used for a seawater challenge test (T in Fig. 1) according to Handeland et al. (2004). In the seawater challenge test, animals were placed in 34 ppt seawater for 96 h and subsequently euthanised. Blood plasma was then analysed for chlorine levels (Cl^-) with a 100 mM Cl^- standard (Titrator: Sherwood 926 s, Sherwood Scientific) to estimate the animals' hypo-osmoregulatory ability in seawater. All remaining animals were PIT-tagged, and radiographed at week 15 (P in Fig. 1). Animals were fed different commercial diets (Skretting, Norway) according to the manufacturer's tables. The diet history groups are hereafter referred to as LP-RP, RP-RP, and HP-RP for animals fed LP, RP, and HP diets in freshwater, respectively. Animals remained fed with the same feeding regime until transfer to seawater at week 18 (Fig. 1). In seawater animals were fed twice a day. Animals were kept in tanks with 1.0 m diameter and subsequently transferred to 3.0 m diameter tanks (Fig. 1). The maximum density in seawater was 87.4 kg/m^3. The temperature and oxygen levels were monitored daily and averaged 11.66 ± 1.02 °C and 97.60 ± 12.50%, respectively. Excess feed was collected once a day by feed collectors with a mesh size of <2 mm to monitor feed intake. All animals were sampled at week 84 (Fig. 1). Nineteen animals died one week after vaccination, three animals died in the 3.0 m diameter tanks, and five animals lost their PIT-tag. These animals were excluded from the analysis.

2.2. Sampling and growth measurements

Animals were measured (fork length) and weighed at week 2, 15, 47, and 84 (Fig. 1). Fulton's condition factor (K) was calculated according to the following equation: $K = (W \times L^{-3}) \times 100$, where W is weight (g) and L is fork length (cm) (Busacker et al., 1990). The specific growth rate (SGR) was calculated as follows: $SGR = (\%\ \text{body mass day}^{-1}) = [(W_{Final}/W_{Initial})^{1/Days} - 1] \times 100$, where $W_{Initial}$ and W_{Final} represent the average animal weight for a given period, and days represent the number of feeding days for that period (Gil Martens et al., 2006). The feed conversion ratio (FCR) was calculated on a dry matter basis (FCR = total feed consumed/ weight gain) (NRC, 2011). Feed intake (g of feed day^{-1}) was recorded daily based on the quantity of recovered feed subtracted from the total daily ration. Both FCR and feed intake were measured in seawater (week 47–84).

2.3. Bone minerals

Vertebrae were dissected, cleaned of excessive muscle, haemal and neural arches and spines were removed, and vertebrae were stored at −20 °C (Drábiková et al., 2021). The samples were rinsed with distilled water (dH_2O). Lipids were removed from the samples in a bath of acetone and methanol (1:1, *v*/v) (2 × 8 h). The samples were dried for 24 h at 105 °C (Witten et al., 2019). The ash cycle consists of 6 h at 100 °C, 3 h at 300 °C, and 4 h at 520 °C. Samples (0.5 g) were wet destructed according to Method III with 4 ml of nitric acid and 12 ml of hydrochloric acid using Digi prep (SCP Science, Canada). The mineral content was measured by inductively coupled plasma atomic emission

Table 1
Growth data. Growth measurements, specific growth rate (SGR), and feed conversion ratio (FCR). Animals were fed either diets containing low (LP), regular (RP), or high dietary phosphorus (HP) for 11 weeks in freshwater. Subsequently Atlantic salmon were fed a diet with regular levels of dietary P (LP-RP, RP-RP, HP-RP). There were no statistically significant differences among measurements ($P < 0.05$).

	Diet group	LP-RP	RP-RP	HP-RP	All animals	*P*-value
Week 2	Weight (g)	13.64 ± 0.97	13.70 ± 1.57	13.12 ± 1.50	13.49 ± 1.50	0.615
	Fork length (cm)	10.46 ± 0.26	10.41 ± 0.43	10.30 ± 0.42	10.39 ± 0.37	0.308
Week 15	Weight (g)	49.74 ± 9.71	50.74 ± 9.50	52.07 ± 7.77	50.85 ± 8.99	0.510
	Fork length (cm)	15.92 ± 0.88	16.11 ± 1.06	16.25 ± 0.89	16.09 ± 0.94	0.163
	Condition factor	1.23 ± 0.13^{a}	1.20 ± 0.07^{b}	1.20 ± 0.08^{b}	1.21 ± 0.09	0.005*
Week 47	Weight (g)	722.32 ± 178.11	732.15 ± 184.54	719.65 ± 158.02	724.71 ± 173.58	0.996
	Fork length (cm)	38.25 ± 2.81	38.01 ± 3.06	38.21 ± 2.59	38.16 ± 2.82	0.814
	Condition factor	1.26 ± 0.09^{b}	1.30 ± 0.09^{a}	1.27 ± 0.10^{ab}	1.28 ± 0.09	0.027*
	SGR (% body mass day^{-1})	1.22 ± 0.11	1.21 ± 0.09	1.20 ± 0.08	1.21 ± 0.09	0.540
	FCR	N/A[1]	N/A	N/A	0.81 ± 0.01	–
	Feed intake (% biomass day^{-1})	N/A	N/A	N/A	1.09 ± 0.01	–
Week 84	Weight (g)	4576.12 ± 1325.74	4620.24 ± 1181.21	4360.74 ± 1180.80	4519.03 ± 1229.25	0.595
	Fork length (cm)	65.00 ± 5.47	65.00 ± 4.40	65.01 ± 4.19	65.00 ± 4.69	0.939
	Condition factor	1.60 ± 0.20^{ab}	1.64 ± 0.19^{a}	1.54 ± 0.21^{b}	1.59 ± 0.20	0.023*
	SGR (% body mass day^{-1})	0.70 ± 0.12	0.70 ± 0.12	0.68 ± 0.15	0.69 ± 0.13	0.941
	FCR	N/A	N/A	N/A	0.92	–
	Feed intake (% biomass day^{-1})	N/A	N/A	N/A	0.88	–

[1]N/A = Not applicable, *Non-parametric Kruskall-Wallis test.

spectroscopy (ICP-OES, Thermo Fisher, Waltham, MA). Ash, Ca, and P content was measured on six abdominal vertebrae from six deformed and six non-deformed animals from LP-RP, RP-RP, and HP-RP groups at week 84 (Fig. 1). Samples were analysed by Masterlab Analytical Services (Nutreco, The Netherlands).

2.4. Radiography

Animals were placed on a 10 MP digital x-ray tablet and radiographed by a portable x-ray unit Gierth TR 90/30 peak (Germany) (www.gierth-x-ray.de). A sample of 36 animals was x-rayed at week 2 to ensure there were no innate deformities at the start of the trial. All animals were x-rayed at week 15 and 47 (Fig. 1). At week 84, all animals were filleted on both sides prior radiography to achieve better resolution of the x-ray images. Radiographs were taken at 80 cm distance between the x-ray source and the tablet at 40 kV, 0.2 mA, and 0.2 s exposure time. Radiographs were analysed as Dicom files using RadiAnt DICOM viewer (Medixant, Poland).

2.5. Vertebral centra deformity diagnosis

Deformities were analysed based on successive digital x-ray images of the same individual animal (Fig. 2, panel A-C). Vertebral column regions were identified following De Clercq et al. (2017b) (Fig. 2, the upper part of the panel A). Types of vertebral deformities were recorded based on Witten et al. (2009). The fusion of one or two vertebrae to the base of the skull (occipital region) or one or two vertebrae to the urostyle are a commonly observed phenomenon with no pathological consequences that occurs in both wild and farmed osteichthyans (Arratia et al., 2001; Arratia and Schultze, 1992; Britz and Johnson, 2005; Clercq et al., 2018; Johanson et al., 2005). These types of fusions were therefore not included in the deformity count.

2.6. Vertebral body morphology

Vertebral columns were fixed in 10% buffered formalin for at least 72 h for subsequent histological and whole mount staining analysis. Vertebral columns were rinsed overnight with tap water, transferred stepwise from 30% to 70% ethanol, and stored in 70% ethanol until further analysis.

2.6.1. Whole mount Alizarin red S staining & maceration

Whole mount Alizarin red S staining for mineralised bone was performed on caudal vertebral bodies (Fig. 1) according to Witten et al. (2019) with the application of 5% KOH in glycerol solution steps. For maceration, vertebrae were brought to dH_2O through a reverse glycerol and dH_2O series (3:1, 1:1, 1:3), subjected to trypsin digestion, and treated with 1% KOH as described in Witten et al. (2005). Vertebral bodies were analysed for their extent of mineralisation and structure of bone trabeculae. Observations on the vertebral column were made using oblique illumination on a Zeiss Axio Zoom V16 Fluorescence Stereo Zoom Microscope equipped with a 5MP CCD camera for imaging.

2.6.2. Histology

Vertebral bodies number 32–35 and 36–39 were dissected for demineralised and non-demineralised serial sections (see Analysis in Fig. 1). For embedding in glycol metacrylate (GMA), samples were transferred stepwise to dH_2O through an ethanol series (50% and 30%), each step lasting for 1 h. Vertebrae allocated for the demineralised sections were submerged in 25% osteomol (Merck, Darmstadt) for 56 h. The solution was renewed once. Samples were subsequently rinsed with running tap water overnight and gradually dehydrated on a rocker for 1 h with graded acetone solutions (30%, 60%, and 100%). The tissue was embedded in GMA according to Witten et al. (2001). An automated microtome (Microm HM360, Prosan) was used to make serial parasagittal and cross sections of 2–9 μm. Sections were stretched on dH_2O mounted and dried at room temperature. Sections were stained with toluidine blue and Von Kossa/Van Gieson (Presnell and Schreibman, 1998), coverslipped with DPX (Sigma-Aldrich), and observed using a Zeiss Axio Imager-Z compound microscope equipped with an Axiocam 503 colour camera.

2.7. Vertebral body measurements

Measurements were taken on digital x-ray images with RadiAnt Dicom Viewer (Fig. 1). Vertebral centrum anterior-posterior length, dorsal-ventral height (radiopaque area), and radiolucent distance (Fig. 2, the lower part of the panel A) were measured on vertebral bodies number 32–41 following Witten et al. (2016).

2.8. Vertebral centrum compression tests

The compression tests were carried out on three animals per tank,

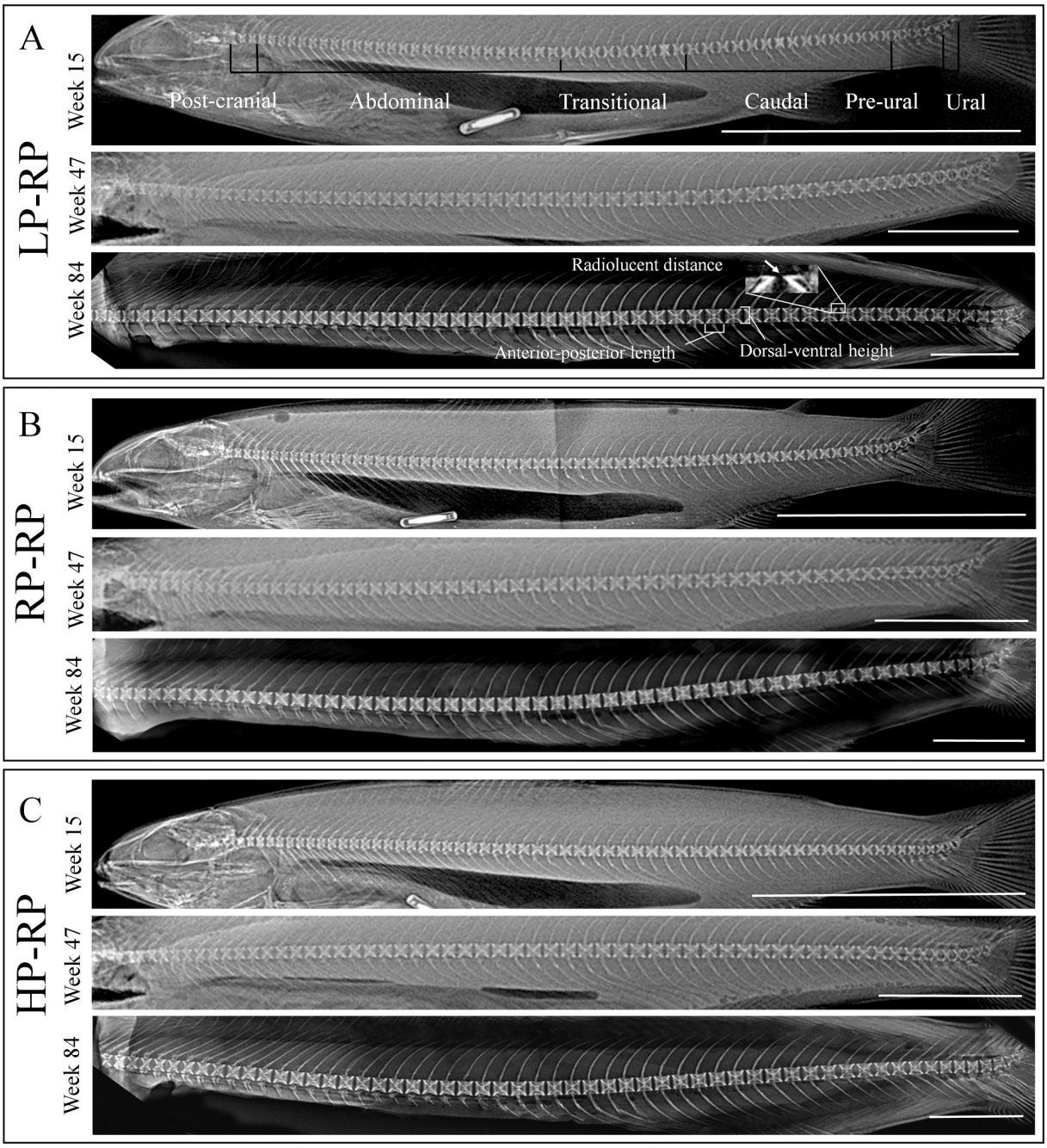

Fig. 2. Radiography. Vertebral columns of three representative animals x-rayed at week 15, 47, and 84. Atlantic salmon were fed diets with low (LP-RP) (panel A), regular (RP-RP) (panel B), and high dietary phosphorus (HP-RP) (panel C) in freshwater. Specimens are oriented anterior to the left and dorsal to the top. The vertebral column regions are indicated in the upper part of panel A. The specimen in panel A had 2, 26, 9, 15, and 5 vertebrae in the post-cranial, abdominal, transitional, caudal, pre-ural, and ural region of the vertebral column, respectively. Anterior-posterior length, dorsal-ventral height of the vertebral centrum (radiodense area), and the radiolucent distance (arrow) used for vertebral centra measurements are indicated in the lower part of panel A. Scale bar = 5 cm.

nine animals per diet history group at the Institute of Marine Research, Matre Research Station, Matredal, Norway. Vertebrae number 43 and 44 which are from the region with higher stiffness and yield load (Fjelldal et al., 2005; 2006) were dissected and stored at −20 °C (Fig. 1). Before the compression tests the vertebrae were thawed, neural and haemal arches and the remains of notochord tissue were removed. Following dissection, vertebral centra were directly measured for anterior-posterior length, dorsal-ventral height, and lateral length diameters to the nearest 0.01 mm using a slide calliper. Load deformity testing was measured with a texture analyser (TA-HD plus Texture Analyser, Stable Micro Systems Ltd., Surrey, UK) by compressing a single vertebral centrum along its anterior-posterior axis with a steadily advancing piston (0.01 mm/s). The test was terminated at 35% compression. The load deformity data was used to calculate the mechanical properties, both not adjusted (Fig. 3A) (Fjelldal et al., 2004) and adjusted for vertebra size/dimensions (Fig. 3B) (Hamilton et al., 1981). Calculations were made using the Texture Exponent Software (Stable Micro Systems Ltd., Surrey, UK). Non-adjusted mechanical properties (stiffness, yield load, and resilience) (Fig. 3A) were calculated according to Fjelldal et al. (2004). Size/dimension adjusted mechanical properties (modulus of elasticity, yield point, failure point, and toughness) (Fig. 3B) were calculated using a modified version of Hamilton

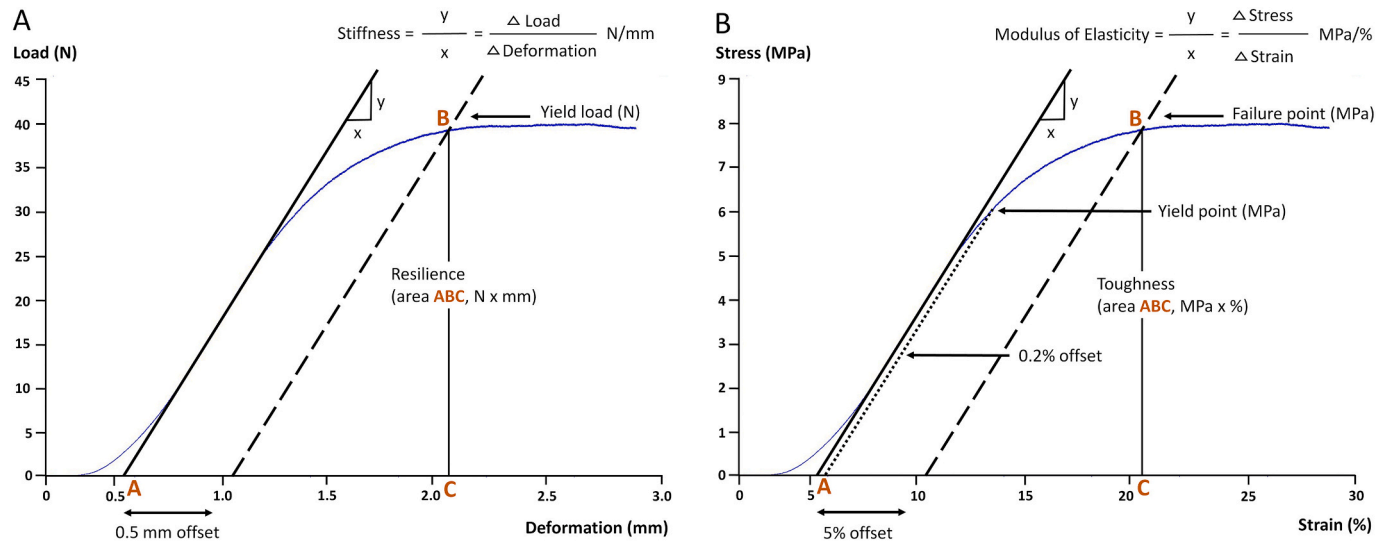

Fig. 3. Load-displacement (A) and stress-strain (B) curves for Atlantic salmon vertebra. Graph (A) shows the relationship between the deformation in millimetre (x-axis) and the load in Newton (y-axis). The blue curve represents the raw load-deformation data. The stiffness (N/mm), defined as the gradient of the initial nearly linear portion of the curve (solid black line), was calculated. The yield load (N) was defined as the load at the intersection between the curve and a 0.5 mm offset line (dashed line), parallel to the initial linear portion of the curve. The area ABC represents the resilience (N x mm) and expresses the ability of the vertebral centrum to absorb energy (adapted from Fjelldal et al., 2004). Graph (B) shows the relationship between the deformation in percentage - strain (x-axis) - and the stress in MPa (y-axis). The blue curve represents the raw stress-strain data. The modulus of elasticity (MPa/%) was calculated as the gradient of the initial nearly linear portion of the curve (solid black line). The yield point (MPa) was defined as the stress at the intersection between the curve and a 0.2% offset line (1st dashed black line), parallel to the initial linear portion of the curve. The failure point (MPa) was defined as the stress at the intersection between the curve and a 5% offset line (2nd dashed black line), parallel to the initial linear portion of the curve. The area ABC represents the toughness (MPa x %) and expresses the ability of the vertebral centra to absorb energy. (For interpretation of the references to colour in this figure legend, the reader is referred to the web version of this article.)

et al. (1981), where the yield point was determined by a 0.2% offset line (Turner, 2006), and the failure point was determined by a 5% offset line. The selection of 5% offset was based on Fjelldal et al. (2004) where a 0.5 mm offset was used on vertebrae that were 10 mm in length. This offset approach was used in order to standardise the measurements and make a direct comparison with future studies possible.

2.9. Statistical analyses

All data are given as mean ± standard deviation. The data were analysed with a one-way ANOVA followed by Tukey's *post hoc* test (Bonferroni corrected) or Kruskal-Wallis test with pairwise *post hoc* comparisons (Bonferroni corrected). The unilaterality of HDV was assessed by means of a chi-squared test of independence. If observed frequencies were less than 5, the Fisher's exact test was preferred. The SPSS software was used for the statistical analysis (Version 28, IBM Corp., USA). Individual animals were considered as statistical replicates. For feed intake and FCR tanks were considered as statistical replicates. The level of statistical significance was set at $P \leq 0.05$.

3. Results

3.1. Growth data

There were no significant differences in growth parameters apart from the condition factor that differed marginally among the diet history groups (Table 1). The average weight at week 2 was 13.49 ± 1.50 g and fork length was 10.39 ± 0.37 cm. At week 15, the average weight was 50.85 ± 8.99 g and the average fork length was 16.09 ± 0.94 cm. The condition factor increased in the LP-RP group (1.23 ± 0.13) compared with RP-RP (1.20 ± 0.07) and HP-RP (1.20 ± 0.08) groups. At week 47, the weight, fork length, condition factor, and specific growth rate (SGR) averaged 724.71 ± 173.58 g, 38.16 ± 2.82 cm, 1.28 ± 0.09, and 1.21 ± 0.09% of biomass day^{-1}, respectively. The condition factor was slightly higher in RP-RP group (1.30 ± 0.09) compared with LP-RP (1.26 ± 0.09). The average value for FCR and feed intake was 0.81 ± 0.01 and 1.09 ± 0.01% of biomass day^{-1}, respectively. At week 84, the average weight for all groups was 4519.03 ± 1229.25 g, the average fork length measured 65.00 ± 4.69 cm, the average condition factor was 1.59 ± 0.20, and the average SGR was 0.69 ± 0.13% body mass day^{-1}. The condition factor was increased in RP-RP group (1.64 ± 0.19) compared with HP-RP group (1.54 ± 0.21). The FCR averaged 0.92 and the feed intake averaged 0.88% of biomass day $^{-1}$ (Table 1).

3.2. Vertebral centra deformities

Vertebral centra deformities in PIT-tagged animals that were x-rayed at three time-points were classified into four categories: (1) recovery, (2) containment, (3) progression, and (4) late-onset. Deformities in the recovery (category 1) negatively affected the vertebral centra but intervertebral joints remained non-deformed. In contrast, in the categories (2), (3), and (4) containment, progression, and late-onset, both vertebral centra and intervertebral joints, were deformed.

3.2.1. Recovery - hyper-dense vertebrae

At week 15, HDV were present in 26 out of 45 LP-RP, 3 out of 45 RP-RP, and 2 out of 45 HP-RP animals (Fig. 4). The number of HDV per animal ranged from one to four. The most commonly affected regions of the vertebral column were the transitional and the anterior caudal region (24 out of 31 animals with HDV). Whole mount Alizarin red S stained specimens of HDV showed a unilateral anterior-posterior compression of the left side of the vertebral centra (Fig. 5A-B). The anterior-posterior compression was present in 15 out of 31 animals with HDV. The left side of HDV showed bent bone trabeculae, more haphazardly organised, with a generally more dorsal-ventral orientation (Fig. 5A). On the right side of HDV and in non-HDV the major bone trabeculae had a regular anterior-posterior direction with narrower bridging between the larger trabeculae (Fig. 5B). Serial histological sections showed bent bone trabeculae, and bone marrow spaces filled with ectopic cartilage (triangles in Fig. 5C-D, black asterisks in Fig. 5E, I-

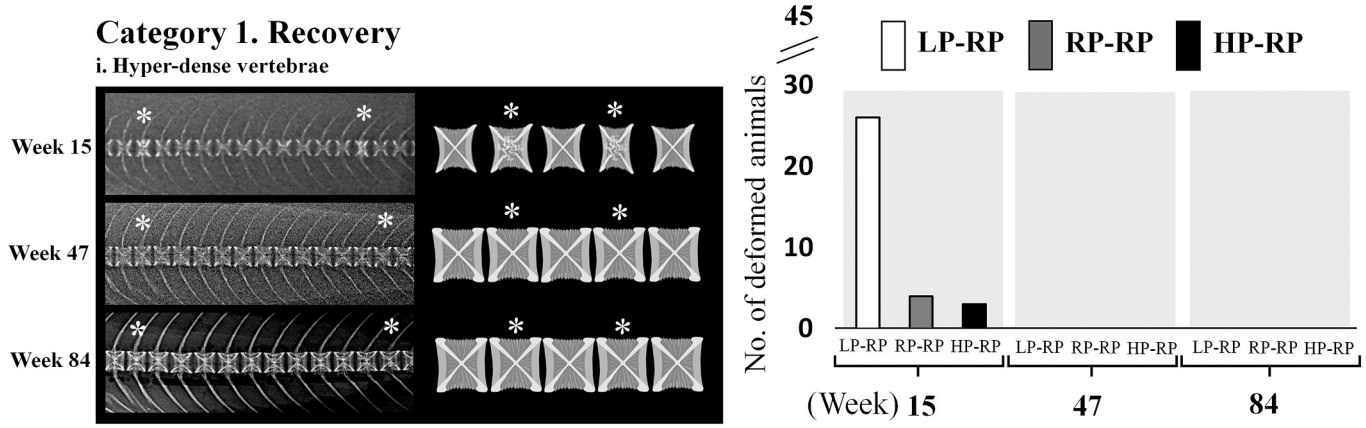

Fig. 4. Hyper-dense vertebrae (HDV). X-ray images and schematic illustrations of a single Atlantic salmon with a low phosphorus diet history at week 15, 47, and 84. Specimens are oriented anterior to the left and dorsal to the top. Asterisks highlight HDV in the animal at week 15 and recovered HDV in the same animal at week 47. The same vertebrae remained non-deformed till week 84 (asterisks). The graph demonstrates prevalence of HDV in animals with a low (LP-RP), regular (RP-RP), and high dietary phosphorus (HP-RP) history at the specified time-points. An increased prevalence of HDV was observed among animals with LP-RP history. All observed HDV recovered at week 47 and remained non-deformed till week 84.

J, L). Ectopic cartilage filled bone marrow spaces were present on the left side of the vertebrae (black asterisk in Fig. 5E, asterisk in Fig. 5J). There was a statistically significant association between unilaterality and HDV deformity in specimens analysed by whole mount Alizarin red S and by series of histological sections ($P < 0.001$). The right side remained non-deformed with bone marrow spaces filled with adipose tissues (Fig. 5F, rectangle in Fig. 5J) comparably to non-HDV (Fig. 5G-H, K). The ectopic cartilage was not observed to be mineralised (triangles in Fig. 5C). Regular cartilage was present at the bases of ribs and neural arches (white asterisks in Fig. 5E-G, J-K). The intervertebral joints remained intact in all animals with HDV (IJ in Fig. 5E-F). The analysis of serial histological sections of seawater recovered HDV showed that the micro-anatomy of the vertebral centrum in recovered HDV was comparable to vertebrae without a HDV history (Fig. 5M-P). Recovered HDV had regular anterior-posteriorly oriented bone trabeculae and bone marrow spaces filled with adipose tissue (Fig. 5O-P). The surface of bone trabeculae in recovered HDV was smooth.

3.2.2. *Recovery - low-mineralised vertebrae*

Low-mineralised vertebrae were present throughout the vertebral column in all 45 LP-RP animals at week 15 (Fig. 6A) due to the presence of non-mineralised bone matrix (Drábiková et al., 2021). All vertebrae were mineralised by week 47 (Fig. 6A).

3.2.2.1. Vertebral body measurements. At week 15, measurements of the radiodense area of the vertebral body on digital x-rays showed significantly shorter anterior-posterior length in LP-RP compared with RP-RP, and HP-RP animals ($P = 0.03$) (Fig. 6B). The radiolucent distance in-between the vertebral centra was significantly extended in LP-RP animals in comparison to the radiolucent distance in RP-RP and HP-RP animals ($P = 0.002$) (Fig. 6B). The dorsal-ventral height and the sum of the anterior-posterior length of the mineralised part of vertebral centra and the radiolucent distance were similar among animals from all diet groups. At week 84, all measurements were comparable in all groups (Fig. 6C).

3.2.2.2. Mineral content analysis - vertebrae. The mineral content analysis of vertebrae at week 84 showed similar ash, calcium, and phosphorus values for deformed and non-deformed animals from all groups (Table 2). There were no obvious differences in the Ca:P ratio among the diet groups, despite a difference in Ca:P ratio between non-deformed RP-RP animals and deformed HP-RP animals. This difference was statistically significant ($P = 0.021$) (Table 2). The ratio of Ca:P in all groups of animals was comparable (Table 2).

3.2.2.3. Bone mineralisation. Digital x-ray images and Alizarin red S stained specimens at week 84 demonstrated well-mineralised vertebral bodies in all three groups (Fig. 7A-F). Similarly to RP-RP and HP-RP animals, the distal ends of the vertebral body endplates in the LP-RP group showed a regular thin layer of non-mineralised bone (osteoid) (Fig. 7G-I). The analysis of non-demineralised sections of the vertebral body endplates showed a comparable level of mineralisation in the three groups with no signs of low-mineralised bone in LP-RP group (Fig. 7J-L).

3.2.2.4. Measurements and mechanical properties of vertebral centra. There were no statistically significant differences in the vertebral centra anterior-posterior length, lateral diameter, and dorsal-ventral diameter of vertebrae which were used for the mechanical properties analysis at week 84 (Table 3). Mechanical properties analysis corrected for size of the vertebral centra showed that the yield-point and toughness of vertebral centra was significantly reduced in HP-RP animals compared with RP-RP animals ($P = 0.047$). The remaining properties corrected and not corrected for size of the vertebral centra were not significantly different among the groups (Table 3).

3.2.2.5. Ectopic cartilage in non-hyper-dense vertebrae. Serial histological sections revealed that the vertebral body endplates were straight and intervertebral ligaments and spaces were well-developed in all diet groups at week 84 (Fig. 8A-C, E, H-I). Areas between the distal part of the vertebral body endplates and the bone trabeculae that were previously occupied by bands of ectopic cartilage in LP animals at week 13 (red arrowheads and red rectangle in Fig. 8D, red arrowhead in F) now showed absence of cartilage. Occasionally dispersed cartilaginous cells, that likely represent a vestige of the former cartilage, were observed (white rectangle in Fig. 8E, white arrowhead in G). Osteoblasts in the vertebral body growth zone were spindle-shaped in all analysed animals (arrowheads in Fig. 8J-L). Sharpey's fibres, the continuation of collagen type I fibre bundles inside the bone, were well-developed in all animal groups (black arrows in Fig. 8J-L).

3.2.3. *Recovery - vertical shift and mild compressions*

A vertical shift deformity was present in 1 out of 45 RP-RP animals and 2 out of 45 LP-RP animals at week 15 (Fig. 9A). Based on x-ray images two adjacent vertebral centra on both sides of the vertically shifted vertebra had a mild one-sided compression (Fig. 9A). Mild compressions were present in 2 out of 45 RP-RP animals at week 15

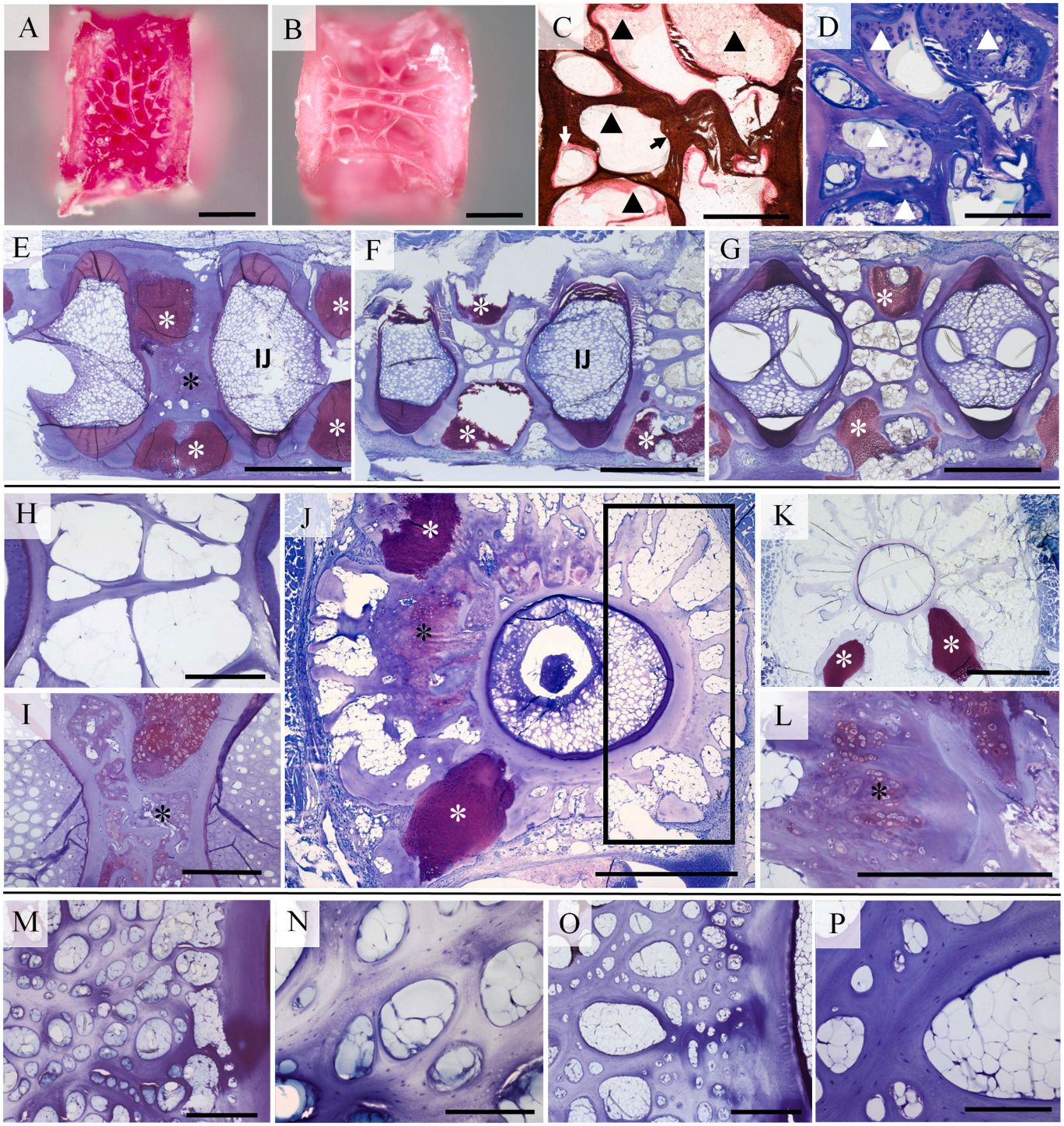

Fig. 5. Morphology of hyper-dense vertebra (HDV). (A-B) Whole mount Alizarin red S stained specimen of freshwater Atlantic salmon vertebra (week 13), scale bar = 1 mm. (C-D) Non-demineralised parasagittal sections, (*E*-I) demineralised parasagittal sections, and (J-L) demineralised cross-sections of freshwater (week 13) Atlantic salmon vertebrae. (M-P) Demineralised parasagittal section of seawater (week 84) Atlantic salmon vertebrae. (C-D) Von Kossa/Van Gieson staining and (E-T) toluidine blue staining, scale bar C-D, H-I, L, N, $P = 250$ μm, E-G, J-K, M, O = 1 mm. (A) The left side of HDV with unilateral anterior-posterior compression of the vertebral centrum with bent and compact bone trabeculae, some in dorsal-ventral orientation. (B) The right side of the same HDV with bone trabeculae orientated in anterior-posterior direction. (C-D) Two images of the same region of the vertebral centrum. Regions of mineralised (black arrow in C), and non-mineralised (white arrow in C) bone trabeculae, and cartilage filled bone marrow spaces are present (triangles in C, D). (E) The left side of HDV with ectopic cartilage filled bone marrow spaces (black asterisk). (F) The right side of the same HDV with bone marrow spaces filled with adipose tissue. (G, H, K) Representatives of non-HDV with regular bone trabeculae and bone marrow spaces filled with adipose tissue. (I, L) Detailed depictions of ectopic cartilages filled bone marrow spaces and bent bone trabeculae. (J) Cross-section of a HDV clearly shows that ectopic cartilage occupies the left side of HDV (asterisk) while the right side of HDV remains non-deformed (rectangle). Intervertebral joints (IJ) in HDV remain intact (E-F). Regular cartilages at the bases of ribs and neural arches are shown (white asterisks in E-G, J, K). The structure of bone trabeculae in a vertebra without HDV history (P-R) and a recovered HDV (S-T) are comparable. Bone surfaces are smooth and without signs of enhanced bone resorption (S-T). (For interpretation of the references to colour in this figure legend, the reader is referred to the web version of this article.)

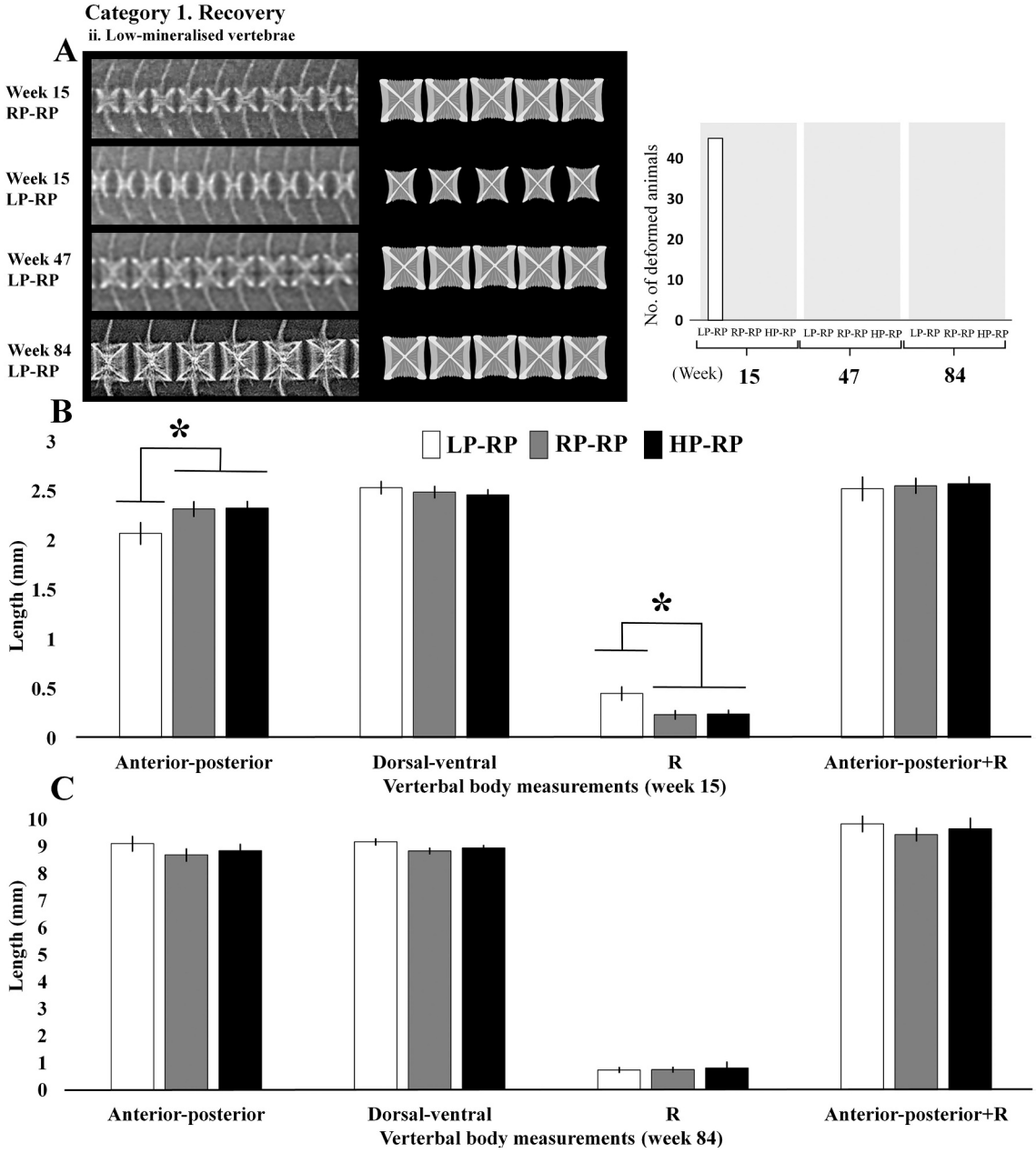

Fig. 6. Low-mineralised vertebrae. (A) X-ray images and schematic illustrations of vertebrae from an animal with regular phosphorus (P) diet history (RP-RP) at week 15 and a single animal with low-P history (LP-RP) at week 15, 47, and 84. Specimens are oriented anterior to the left and dorsal to the top. The graph in panel A demonstrates the prevalence of low-mineralised vertebrae in LP-RP animals examined at week 15 and the absence of low-mineralised vertebrae at all other time-points and in all other diet groups. (B, C) Vertebral length (anterior-posterior), vertebral height (dorsal-ventral), radiolucent distance (R) were measured at week 15 (B) and at week 84 (C) from ten consecutive vertebral bodies number 32–41 of six animals per group. Animals had a history of LP, RP, and high dietary P (HP-RP) for 11 weeks in freshwater (week 2–13) with a subsequent period of regular levels of dietary P. Significant differences among the groups are denoted by an asterisk. Anterior-posterior length in LP-RP at week 15 was significantly reduced compared with the anterior-posterior length in RP-RP and HP-RP animals (one-way ANOVA, $P = 0.03$) (B). Radiolucent distance in LP-RP at week 15 was significantly increased relative to radiolucent distance in RP-RP and HP-RP animals (one-way ANOVA, $P = 0.002$) (B). There were no significant differences in dorsal-ventral height at week 13 (B) and in all the vertebral body measurements among animals at week 84 (C).

(Fig. 9B) in the abdominal vertebral region. These animals had two vertebral centra affected by one-sided compression and one by homogenous compression. Both vertical shift and mild compressions were observed to recover at week 47 and remained non-deformed till week 84 (9A-B).

3.2.4. *Containment – stabilisation of vertebral fusion*

Vertebral fusions could be stabilised by remodelling of two or three vertebral bodies into one regularly shaped vertebra, here designated as containment (category 2). Also, those vertebrae that are in the process of fusion were assigned to this category. At week 15, 7 out of 45 LP-RP, 6 out of 45 RP-RP, and 4 out of 45 HP-RP animals were observed with a vertebral fusion in a process of stabilisation (Fig. 9C). At week 47, one additional animal in RP-RP, two animals in HP-RP, and five animals in LP-RP group developed a compression which at week 84 progressed into a vertebral fusion (graph in Fig. 9C). Stabilisation of vertebral fusion was observed at all three time-points and at all stages of fusion: initial stage of compression (Fig. 9C ii.), advanced stage of fusion (Fig. 9C i.), and a final stage represented by a remodelled stable vertebral fusion (Fig. 9C iii.).

Table 2
Mineral analysis of vertebrae. Values show the content of ash, calcium (Ca), phosphorus (P) (% of wet weight), and Ca:P ratio in six vertebrae from the abdominal region of animals at week 84 with low (LP-RP), regular (RP-RP), and high (HP-RP) dietary phosphorus in the freshwater (week 2–13) with a subsequent period on a RP diet. Six deformed (D) and non-deformed (N) animals were analysed per group. The statistical significance ($P < 0.05$) is denoted by a different lowercase superscript (within a row).

Diet group	LP-RP		RP-RP		HP-RP		All groups	*P*-value
	N	D	N	D	N	D		
Ash (%)	32.35 ± 1.76	29.53 ± 1.31	31.45 ± 2.36	30.25 ± 1.67	30.75 ± 1.70	31.08 ± 1.82	30.90 ± 1.94	0.102
P (%)	5.51 ± 0.29	5.13 ± 0.29	5.51 ± 0.39	5.26 ± 0.33	5.17 ± 0.25	5.26 ± 0.32	5.31 ± 0.33	0.237
Ca (%)	11.28 ± 0.60	10.47 ± 0.60	11.43 ± 0.81	10.72 ± 0.73	10.49 ± 0.54	10.62 ± 0.69	10.84 ± 0.71	0.085
Ca:P	2.05 ± 0.01^{ab}	2.04 ± 0.01^{ab}	2.07 ± 0.02^{a}	2.04 ± 0.03^{ab}	2.03 ± 0.02^{ab}	2.02 ± 0.01^{b}	2.04 ± 0.02	0.021*

* Non-parametric Kruskall-Wallis test.

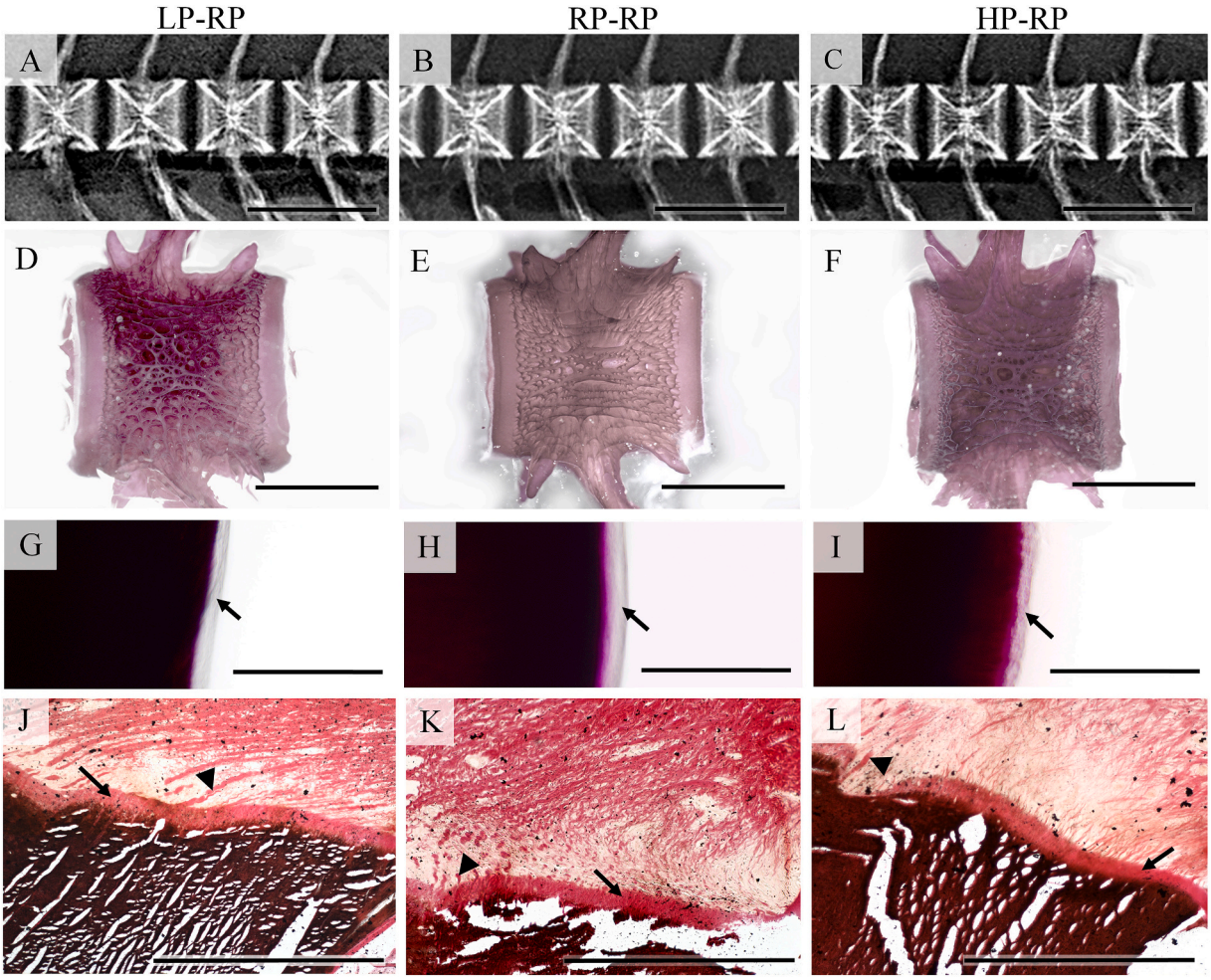

Fig. 7. Mineralisation of low-mineralised vertebrae. (A-C) X-ray images, scale bar = 1.5 cm, (D-I) whole mount Alizarin red S stained specimens, scale bar D-F = 5 mm and G-*I* = 250 μm. (J-L) Non-demineralised histological sections of vertebral body endplates of representative animals with a low (LP-RP), regular (RP-RP), and high phosphorus (HP-RP) diet history in freshwater (week 84). Von Kossa/Van Gieson, scale bar = 500 μm. The specimens are oriented anterior to the left and dorsal to the top. (A-F, J-K) Display vertebral bodies in parasagittal plane and (G-I) display a part of the vertebral body in transverse plane. The level of mineralisation in vertebral bodies in LP-RP animals (A, D, G, J) is comparable to the level in RP-RP (B, E, H, K) and in HP-RP (C, F, I, L). Atlantic salmon of all groups display a regular thin layer of osteoid (non-mineralised bone) at the outer edge of the vertebral centra (arrows in G-I) and at the edges of the vertebral body endplates (arrows in J-L). The bone trabeculae are oriented in regular anterior-posterior direction in all diet groups (D-F). The arrowheads in J-L point to Sharpey's fibres (see also Fig. 8, J-C). (For interpretation of the references to colour in this figure legend, the reader is referred to the web version of this article.)

3.2.5. Progression - compressions and progressive vertebral fusion

Progression (category 3) included compressions and progressive vertebral fusion. Mild (one-sided) compressions affecting two to five vertebral centra (asterisks in Fig. 10A) occurred in 3 out of 45 LP-RP animals at week 47 (graph in Fig. 10A). At week 84, the deformities remained mild or progressed into the initial stages of vertebral fusion indicated by a radiodense (*i.e.* mineralised) area between two vertebral centra (arrows in Fig. 10A). One out of 45 RP-RP and HP-RP animals, and 2 out of 45 LP-RP animals had progressive vertebral fusion throughout the study (asterisks and graph in Fig. 10B). The average number of fused and compressed vertebral centra was seven. Compressions were observed in the transitional and caudal regions while progressive vertebral fusion were observed in the abdominal and transitional region (area below the dorsal fin).

Table 3
Measurements and mechanical properties of vertebral centra. Vertebral (V) anterior-posterior length, V lateral diameter, V dorsal-ventral diameter were measured. Analysed mechanical properties were corrected for size of the vertebral centra and not corrected for size of the vertebral centra. Nine animals were measured at week 84 with a low (LP-RP), regular (RP-RP), and high (HP-RP) dietary phosphorus history in the freshwater (week 2–13) with a subsequent period with a RP diet. The statistical significance ($P < 0.05$) is denoted by a different lowercase superscript (within a row).

Diet group	LP-RP	RP-RP	HP-RP	*P*-value
V anterior-posterior length (mm)	9.39 ± 0.73	8.93 ± 0.72	9.01 ± 0.31	0.390
V lateral diameter (mm)	11.50 ± 0.87	10.63 ± 0.84	10.86 ± 0.65	0.155
V dorsal-ventral diameter (mm)	9.80 ± 0.64	9.22 ± 0.74	9.26 ± 0.32	0.170
Mechanical properties (corrected for size of the vertebral centra)				
Modulus of elasticity (MPa/%)	0.62 ± 0.04	0.67 ± 0.03	0.68 ± 0.05	0.206
Yield-point (MPa) (0.2% offset)	5.21 ± 0.52^{ab}	5.48 ± 0.42^{a}	4.56 ± 0.45^{b}	0.047*
Failure point (MPa) (5% offset)	7.26 ± 0.27	7.80 ± 0.25	7.04 ± 0.10	0.089
Toughness (MPa x %)	78.57 ± 6.44^{ab}	82.84 ± 6.08^{a}	69.62 ± 4.19^{b}	0.047*
Mechanical properties (not corrected for size of the vertebral centra)				
Stiffness (N/mm)	560.92 ± 41.01	571.50 ± 18.43	571.13 ± 37.78	0.589
Yield-load (N) (0.5 mm offset)	651.38 ± 24.89	612.87 ± 7.82	557.97 ± 4.29	0.338
Resilience (N x mm)	702.47 ± 43.55	609.45 ± 24.31	533.05 ± 22.71	0.158

* One-way ANOVA.

3.2.6. *Late-onset - vertical shift, compressions and fusions*

Late-onset (category 4) deformities were found in the posterior transitional and the caudal region and included vertical shift, compressions and fusions (asterisks in Fig. 10C). Late-onset vertical shift negatively affected both vertebral centra and intervertebral spaces. Two to five vertically shifted vertebrae were found in 3 out of 45 RP-RP and in 4 out of 45 LP-RP and HP-RP animals at week 84 (graph in Fig. 10C). Late-onset compressions and fusions were observed as one-sided compression, as homogenous compressions, and as compressions with fusions (asterisks in Fig. 10D) in 5 out of 45 RP-RP, 4 out of 45 HP-RP, and 2 out of 45 LP-RP animals (graph in Fig. 10D). Animals had up to 14 consecutive deformed vertebral centra in groups of two vertebrae.

4. Discussion

This study assessed the development, progression, and regression of vertebral deformities in 135 individually PIT-tagged Atlantic salmon from week 15 (pre-smolts) to week 84 (harvest), allowing to monitor possible changes in the vertebral column in individuals over time. The study also analysed the long-term effect of a period of low, regular, and high dietary P during the animals' freshwater phase. A surprising finding of this study is the potential of several types of deformities to regress or to stabilise during the animals' seawater phase which could be observed as a result of following individual animals. Deformities that regress or stabilise may not constitute a major problem for animal welfare or product quality at harvest. Strikingly, deformities in which the intervertebral joints remain intact have the potential to recover differently from those that affect both vertebral centra and intervertebral joints. Deformities where intervertebral joints remain intact include hyperdense vertebrae (HDV), initial stages of compressed vertebrae, and vertical shifts. The experimental conditions which included minimum handling stress and stable water temperature, possibly contributed to the observed recoveries. Deformities that affected both the centra and intervertebral joints were stable vertebral fusions, progressive vertebral fusions, late-onset fusions, and late-onset vertical shifts. Interestingly, this study and studies by Sambraus et al. (2014) and Witten et al. (2006) show that fusions cannot recover but can be contained and remain stable, in which case they do not represent a chronic welfare issue. Likewise, late-onset deformities (developed within the last 37 weeks prior to harvest) such as late-onset vertical shifts and initial stages of compression or fusions were found to remain benign. Interestingly, this study showed that the number of progressive and late-onset deformities was not associated with the dietary P levels in freshwater.

A curious finding of this study was the high abundance of hyperdense vertebrae (HDV) at week 15 and the subsequent absence of all identified HDV in the same animals at week 47. This is a notable example of a vertebral deformity which disappears rather than progresses and worsens over time. In Atlantic salmon HDV is a frequent radiologically diagnosed deformity (Helland et al., 2006; Fraser et al., 2019; Sambraus et al., 2020; Ytteborg et al., 2016). Here it is shown that while vertebral centra in HDV are affected, the intervertebral joints remain non-deformed. In this study, HDV were detected in 26 out of 45 LP-RP pre-smolts with a low-mineralised vertebral body phenotype. This is in accord with findings of Helland et al. (2006), a study that also associates the presence of HDV with mineral deficiency, albeit related to phytic acid as a dietary ingredient. HDV are identified based on increased radiodensity. As shown in this study and in study by Helland et al. (2006) the increased radiodensity likely relates to ectopic cartilage that has replaced the adipose tissue in bone marrow spaces and bent and compact bone trabeculae due to anterior-posterior compression.

The findings of this study show that HDV has a unilateral occurrence. All analysed representative samples of Alizarin red S whole mount stained specimens and serial histological sections showed that the ectopic cartilage and bent bone trabeculae occupied the left side of the vertebra. The right side remained non-deformed with well-structured bone trabeculae and adipose tissue inside the bone marrow spaces. Although Helland et al. (2006) did not comment on the unilaterality of ectopic cartilage and bent bone trabeculae, the occurrence of these structures is documented for the left side. This study and the study by Helland et al. (2006) found HDV commonly located in the transitional and the anterior caudal region of the vertebral column. The unilateral occurrence could be related to compression due to muscles exerting mechanical load on the left side of the vertebrae of the transitional and anterior caudal regions caused by anti-clockwise swimming in tanks with limited diameters. This is comparable to the development of lordotic vertebrae in European sea bass as an adaptation to increased mechanical load in high water current velocity (Kranenbarg, 2005; Kranenbarg et al., 2005). In Atlantic salmon, the transitional and anterior caudal regions are subjected to an increased mechanical load during swimming and thus show the highest stiffness in the vertebral column (Fjelldal et al., 2004). Atlantic salmon is a sub-carangiform swimmer which can explain both the increased mechanical load and the stiffness of transitional and anterior caudal vertebrae. Sub-carangiform swimming generates a forward swimming force by limited anterior body undulation and increased undulation of the posterior half of the body (Sfakiotakis et al., 1999). Moreover, Atlantic salmon and rainbow trout (*Oncorhynchus mykiss*) swimming against a stronger current were shown to have increased vertebral body mineralisation and increased stiffness in the transitional and anterior caudal regions (Deschamps et al., 2009; Solstorm et al., 2016; Totland et al., 2011). Compression is a factor that initiates the conversion of connective tissue into cartilage (Hall and Witten, 2019; Pauwels, 1960; Weinans and Prendergast, 1996). Thus, the occurrence of ectopic cartilage in HDV can possibly be attributed to the continuous compression forces on the left side of the vertebral centra during anti-clockwise swimming. Interestingly, studies by Berge et al. (2009), Helland et al. (2006), Fjelldal et al. (2016), and Fraser et al. (2019) also observed HDV in freshwater stages of Atlantic salmon reared in tanks with limited diameters, ranging from 0.5 to 0.6 m. These results,

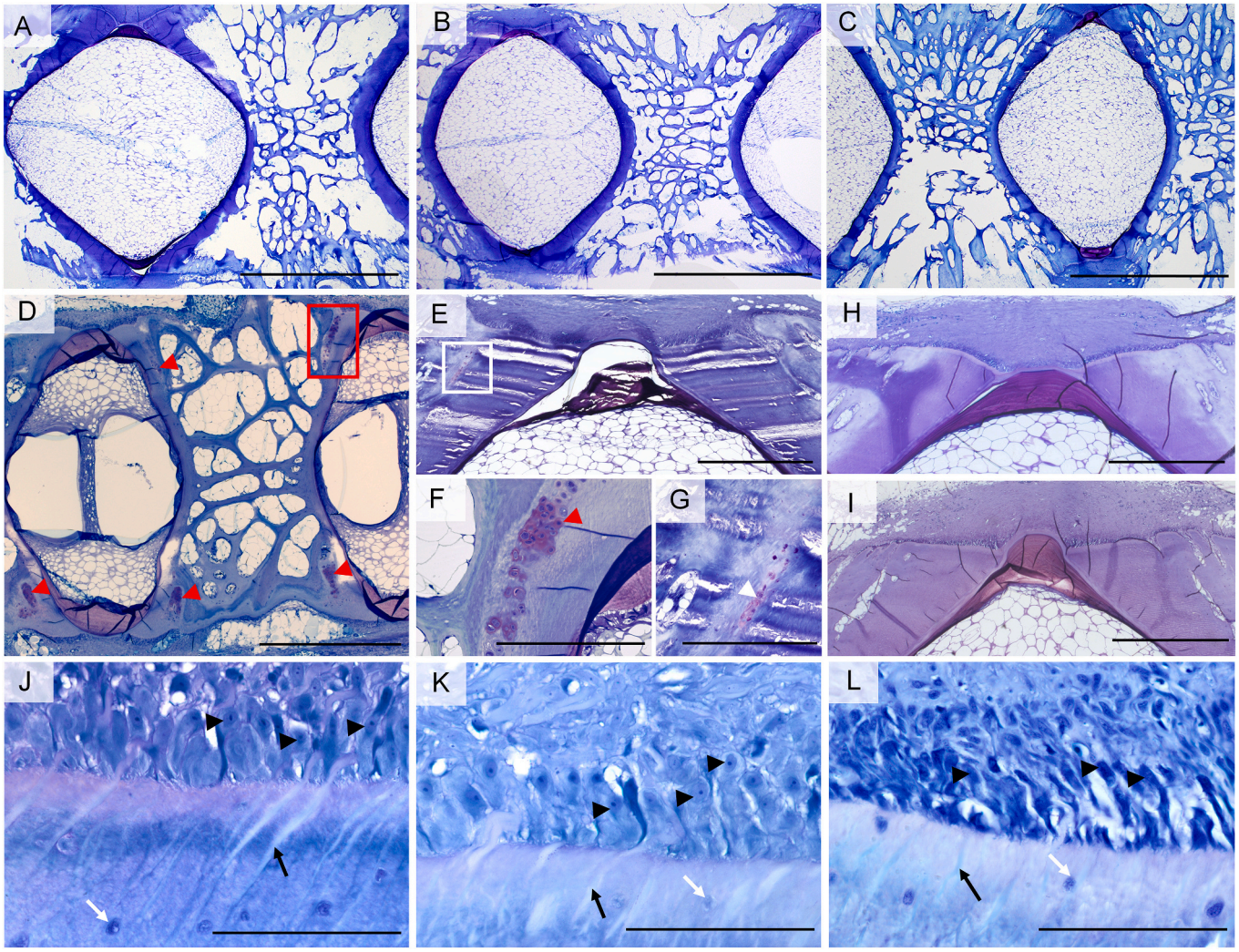

Fig. 8. Morphology of vertebral bodies. Demineralised, toluidine blue stained histological sections representing specimens from Atlantic salmon at week 84 (A-C, E, H-L) and at week 13 (D, F) following an 11 week long feeding trial with low (LP-RP), regular (RP-RP), and high (HP) dietary phosphorus in freshwater. Scale bar A-C = 5 mm, D-E, H-I = 1 mm, and F-G = 500 μm, J-L = 100 μm. Specimens are oriented anterior to the left and dorsal to the top. The intervertebral joints are well-developed and vertebral body endplates are straight in all groups (A-C). Ectopic cartilage between the distal part of the vertebral body endplates and the non-mineralised bone trabeculae was present in the freshwater stages of LP-RP animals (red arrowheads in D, F (magnification of red rectangle in D)). This cartilage was absent or occasionally, cartilaginous cells, a likely vestige of this cartilage, was observed in seawater (white rectangle in E, white arrowhead in G (magnification of white rectangle in E)). Intervertebral ligaments are intact in all three groups (E, H-I). Osteoblasts are in an active form in all groups (arrowheads in J-L). Sharpey's fibres are well-developed (black arrows in J-L). White arrows in (J-L) mark osteocytes. (For interpretation of the references to colour in this figure legend, the reader is referred to the web version of this article.)

in addition to the results of the current study, indicate that a small tank diameter may represent an additional risk factor for HDV development. The absence of HDV in a study by Vera et al. (2019) that raised freshwater stages of Atlantic salmon in tanks with a volume of 1800 *l* lends further support to the suggestion that the commonly used small size tanks could be a factor for HDV development. The unilaterality of HDV is not commonly observed because lateral x-ray images are the basic diagnostic tool for identifying vertebral column deformities. Possibly, other types of vertebral deformities could also be asymmetric. If asymmetry would be a result of tank size and swimming direction, farming practice should pay attention to these parameters.

Baeverfjord et al. (2009) observed that HDV may lead to the development of fusion. This was not observed in the current study where all identified HDV recovered in seawater. Further, all HDV had intact intervertebral joints which could have facilitated the process of recovery as in the case of other recovered deformities in this study. Previous studies show that in teleosts cartilage is removed to give rise to bone marrow spaces (Witten and Huysseune, 2009). As in HDV, cartilage is resorbed and replaced by adipose tissue, which is the normal tissue in teleost bone marrow spaces (Witten and Huysseune, 2009 Fig. 1A, B). In contrast, ectopic cartilage that develops in intervertebral spaces causes a lasting alteration of the joint, changes the growth pattern of the vertebral centra, and can lead to vertebral fusion in a process similar to endochondral bone formation (Witten et al., 2005, 2006). These are possible reasons why vertebral centra deformities with no associated intervertebral joint damage can recover and deformities with damaged intervertebral joints cannot. The recovery of HDV was found to be completed at week 47. The absence of HDV in seawater is in accordance with previous studies which observed HDV in freshwater but not in seawater (Berge et al., 2009; Fjelldal et al., 2016).

Vertical shift, also referred to as light lordosis, dislocation, cross-stitch, slipping vertebra, and deformity type 17, affect single vertebra or multiple consecutive vertebral bodies (Favaloro and Mazzola, 2000; Fjelldal et al., 2004, 2007a; Fragkoulis et al., 2019, 2022; Gil Martens et al., 2012; Holm et al., 2020; Perrott et al., 2018; Trangerud et al., 2020; Witten et al., 2009). In this study, vertical shifts, observed in

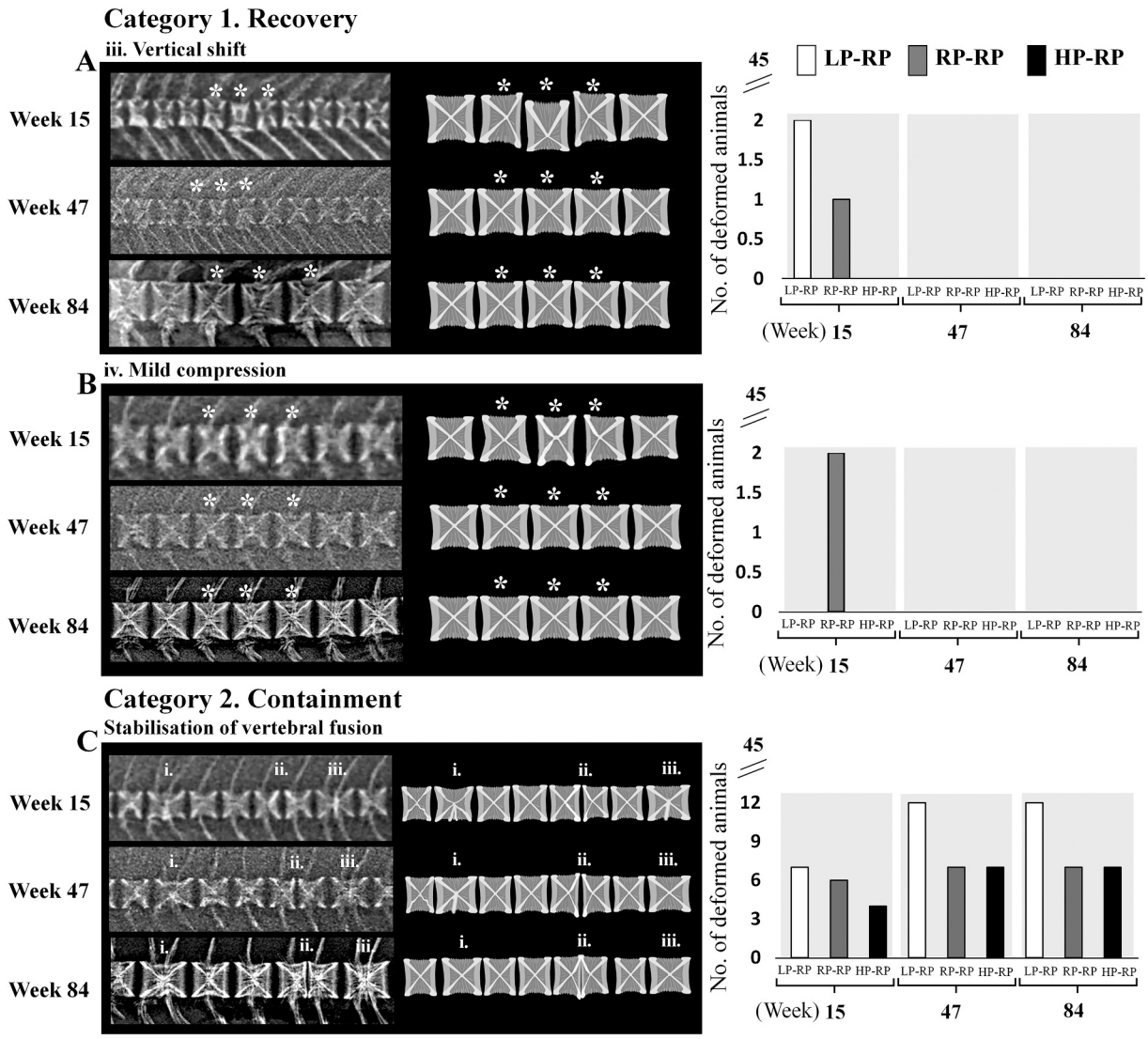

Fig. 9. Vertebral deformity development: recovery and containment. To the left: x-ray images and schematic illustrations of deformities in a single Atlantic salmon at week 15, 47, and 84. Specimens are oriented anterior to the left and dorsal to the top. To the right: the graphs demonstrate the prevalence of the deformity in animals with a low (LP-RP), regular (RP-RP), and high (HP-RP) dietary phosphorus history at the specified time-points. Recovery (category 1) included vertical shift (A) and mild compression (B). The specific deformities and vertebrae recovered from the deformities are marked by asterisks. Containment (category 2) refers to stabilisation of vertebral fusion of up to three vertebrae (C). Stabilisation of vertebral fusion was observed at three stages. From left: (i.) the onset of remodelling of two vertebral centra in stable vertebral fusion, (ii.) the initial stages of a vertebral centra compression (flattened vertebral body endplates), and (iii.) a stable vertebral fusion of two vertebral centra in the process of remodelling. Note: stable vertebral fusion can be identified by the presence of two neural and haemal arches or ribs which are not affected by the fusion process.

freshwater at week 15, affected three vertebral centra while intervertebral joints remained intact. In this study vertical shifts recovered in seawater. The recovery of vertical shifts (*i.e.* light lordosis) was also observed in juvenile sharp snout sea bream, *Diplodus puntazzo*, Gilthead sea bream, and European sea bass (Favaloro and Mazzola, 2000; Fragkoulis et al., 2019, 2022). While 2.5% of examined Gilthead sea bream specimens suffered light lordosis and 10.5% had externally detectable lordosis, 43.6% of the deformed animals reverted to a regular external phenotype. A complete recovery of the vertebral column was observed on radiographs in 14.6% of the recovered individual animals whereas 12.2% retained minor deformities (Fragkoulis et al., 2019 Fig. 6A and B). The remaining 73.2% of animals did not fully recover and showed a light lordosis (48.8%) or a kyphosis to counterbalance the lordosis (24.4%) (Fragkoulis et al., 2019 Fig. 8C and D). In a study on European sea bass, 33% of the juveniles developed a lordotic phenotype. Of these, 60% recovered during the on-growing period (Fragkoulis et al., 2022). In another study, Favaloro and Mazzola (2000) observed lordotic vertebrae in 30% of juvenile sharp snout sea bream while these deformities were absent in adult animals. In European sea bass, lordosis is associated with ectopic bone formation (chondroid bone) at the articular surfaces of the vertebrae as an adaptation to increased loads (Kranenbarg, 2005; Kranenbarg et al., 2005). The recovery of haemal lordosis in Gilthead sea bream and European sea bass was attributed to the reduced water current in the sea cages which alleviated the loads exerted on the vertebral column (Fragkoulis et al., 2019, 2022). A similar recovery scenario could possibly also apply to HDV observed in this study. Perhaps the reduction in mechanical load on HDV following the transfer to larger seawater tanks facilitated the remodelling of the bent bone trabeculae and ectopic cartilage into regularly shaped vertebrae in the seawater.

Late-onset vertical shifts observed in seawater developed *de novo* in the last 37 weeks of this study. Late-onset vertical shifts affected two to five vertebral centra, as well as the intervertebral joints. Farmed Atlantic salmon affected by several consecutive vertically shifted vertebral

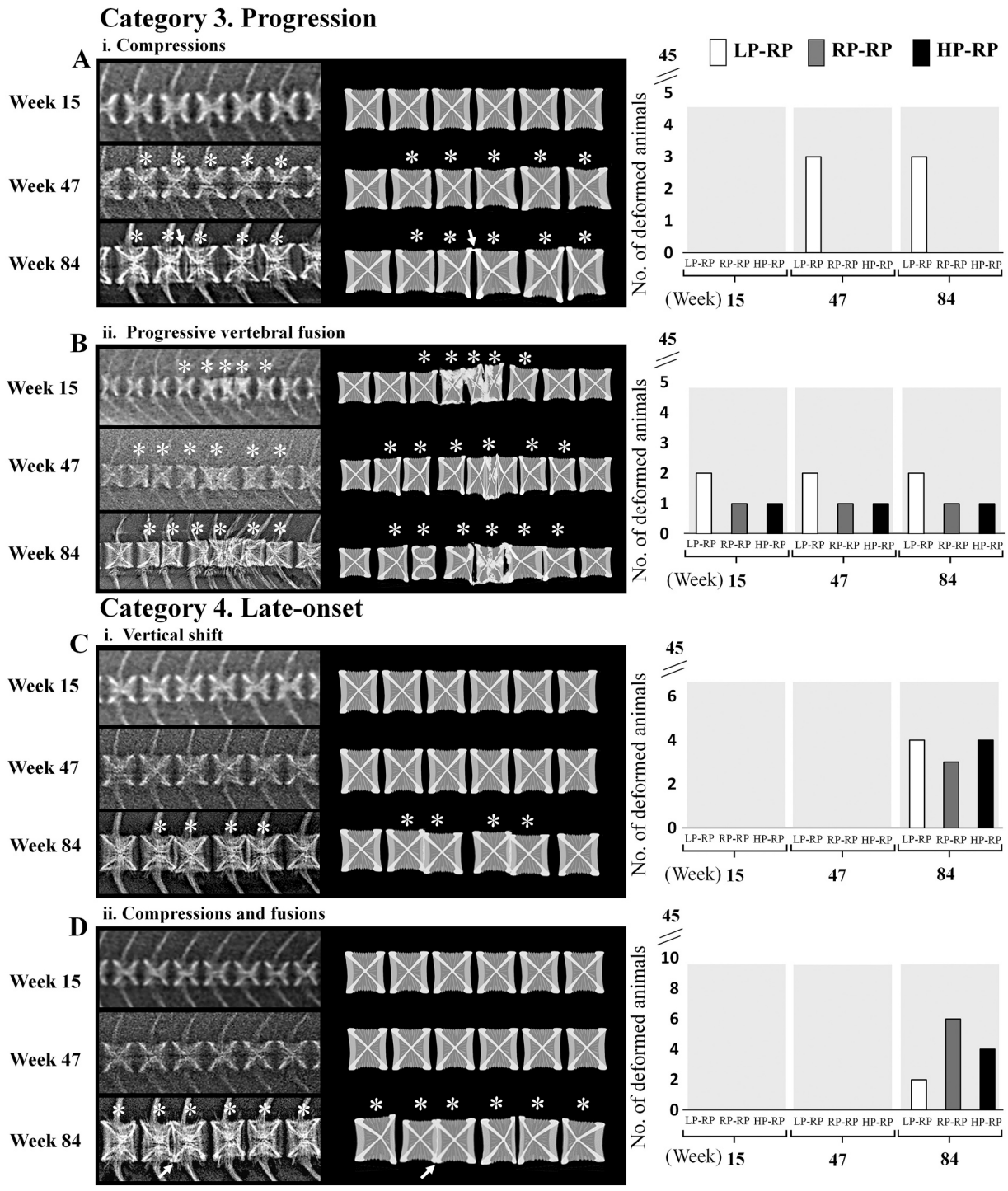

Fig. 10. Vertebral deformity development: progression and late-onset. On the left: x-ray images and schematic illustrations of deformities in a single Atlantic salmon at week 15, 47, and 84. Specimens are oriented anterior to the left and dorsal to the top. On the right: the graphs demonstrate the prevalence of the deformity in animals with a low (LP-RP), regular (RP-RP), and high phosphorus (HP-RP) diet history at the specified time-points. Deformed vertebrae are highlighted by asterisks. Progression (category 3) contained compressions (A) and progressive vertebral fusion (B). Initial stages of compressions (A) were observed at week 47 while the deformity progressed slowly into initial stages of fusion which can be observed by the mineralised (radiodense) area between the vertebral centra (arrow) at week 84. Compressions were observed in the caudal vertebral region. Progressive vertebral fusion (B), a severe type of a progression, already visible at week 15. Here, three vertebral centra are in the process of fusion while two adjacent vertebral centra showed signs of homogenous and one-sided compression. The progression was fast and at week 47 eight vertebrae were visibly deformed (asterisks). At week 84, the vertebral centra consisted of five fusing vertebrae with four adjacent vertebral bodies with one-sided compression. Progressive vertebral fusion were observed in the abdominal vertebral region (below the dorsal fin). Late-onset (category 4) deformities included vertical shift (C) and compressions and fusions (D) which developed between week 47 and 84 in the caudal vertebral region. (C) Shows late-onset vertical shift with fused vertebral body endplates. Here the animal shows two groups of vertically shifted vertebrae. (D) Late-onset compressions and fusions (arrow) affected vertebral centra in groups of two with a maximum of 20 mildly deformed vertebrae per animal.

centra were also reported by Holm et al. (2020) and by Trangerud et al. (2020). This deformity occurs in freshwater (Fjelldal et al., 2007b) and in late seawater stages (Holm et al., 2020; Fjelldal et al., 2004, 2012; 2007a; Trangerud et al., 2020; Witten et al., 2009). Multiple vertically shifted vertebrae observed in freshwater stages of Atlantic salmon were reported to develop into progressive vertebral fusion (Fjelldal et al., 2007a). As has been pointed out by Hansen et al. (2010), low numbers of vertebral deformities in Atlantic salmon have no impact on the animals' health and performance. These deformities were therefore considered as mild phenotypes.

Compression and fusion represent a frequent problem for farmed Atlantic salmon (Fjelldal et al., 2012; Fjelldal et al., 2007a; Witten et al., 2005, 2006, 2009). In line with Witten et al. (2006), this study observed two types of developmental pathways for vertebral fusion: containment (category 2) and progression (category 3). In the current study, initial stages of containment were detected in all life stages. Deformities either remained in the initial stages or progressed towards a stable vertebral fusion. In some cases, initial stages of fusion, *i.e.* vertebral body endplate compression, could also recover. Recovery was only observed in cases where intervertebral joints remained intact. Under the conditions that were used in the current study, it took about 66 weeks for a deformity to develop from an initial stage of fusion into a stable vertebral fusion. This observation is in line with Witten et al. (2006) where vertebral centra of farmed Atlantic salmon with initial stages of fusion became stabilised after 52 weeks in seawater. The presence of stable vertebral fusions already in early freshwater stages suggests that the onset of fusion containment is faster in freshwater compared with seawater. This likely relates to the animals' faster growth in freshwater (Austreng et al., 1987). Stable vertebral fusions of up to three vertebral centra, between post-cranial and ural regions, where the directly adjacent intervertebral spaces and vertebral centra remain non-deformed, have been observed in several farmed and wild salmon species such as Atlantic salmon and Pacific salmon (*Oncorhynchus keta*, *Oncorhynchus gorbuscha*, *Oncorhynchus nerka, O. tshawytscha*) (De Clercq et al., 2017a; Gill and Fisk, 1966; Sambraus et al., 2014). This indicates that stable vertebral fusions are common. A fusion of one to two vertebrae to the occipital region of the skull and fusions of ural and preural vertebral centra have no pathological consequences for the animal and occur regularly as part of normal development in many teleost species (Bensimon-Brito et al., 2012; Britz and Johnson, 2005; Ford, 1937). Indeed, the current study and the studies by Sambraus et al. (2014) and Witten et al. (2006) suggest that stable vertebral fusions of up to three vertebral bodies are frequently encountered variations of the vertebral centra with no pathological consequences.

Progressive vertebral fusions involve more than three adjacent vertebrae and are often associated with ectopic fibrous connective tissue that extends into the muscles (Fraser et al., 2019). In the current study, developing progressive vertebral fusion could be identified in animals prior to seawater transfer. This corresponds with results from Witten et al. (2006); Fig. 1a-c) and Fjelldal et al. (2007a) that observed signs of progressive vertebral fusion in farmed Atlantic salmon prior to seawater transfer. The initial stages of progressive vertebral fusion involve three or more fusing vertebral centra with the adjoining vertebral centra showing signs of compression. Progressive vertebral fusion is likely to worsen with time. Similarly, Fjelldal et al. (2009b) reported progressive vertebral fusion development in Atlantic cod after a year of intensive farming.

Low-mineralised bone in Atlantic salmon parr has been associated with (i) lengthened intervertebral spaces, (ii) thickened intervertebral ligaments, (iii) inward bending of the vertebral body endplates, (iv) ectopic cartilage at the interface between the non-mineralised vertebral body endplates and bone trabeculae, (v) extended areas of non-mineralised bone, and (vi) reduced vertebral centrum stiffness (Drábiková et al., 2021; Helland et al., 2005; Fjelldal et al., 2007b; Witten et al., 2016, 2019; Ytteborg et al., 2016). Histological sections could not reveal LP diet-related structural alterations in LP-RP animals at harvest. Areas with ectopic cartilage at the interface between the non-mineralised vertebral body endplates and bone trabeculae following a P-feeding trial (Drábiková et al., 2021; Witten et al., 2016, 2019) were no longer observed in animals at harvest. Radiographs, bone mineral analysis, Alizarin red S staining, and non-demineralised histological sections showed that animals fully restored their bone mineral content with regular levels of dietary P. Findings by Witten et al. (2019) together with this study indicate that Atlantic salmon, subjected to a limited period of P deficiency in the freshwater or seawater phase, have the potential to recover with a diet containing the required P level with no adverse long-term effects on bone formation, bone mineralisation, and bone mechanical properties.

Different from the bone mineral content measurement, compression tests in vertebral centra of HP-RP animals showed a significant reduction of the average yield point and toughness compared with other groups. The reduced values for the yield point and toughness suggest that the bone in animals with an increased level of dietary P in freshwater can be more brittle in comparison with RP-RP animals. As a consequence, bone of the HP-RP animals is possibly disposed to develop micro-cracks under an increased strain compared with the bone of the other groups (Einhorn, 1992; Hart et al., 2017). Stress (external force) exerted on a bone creates strain (structural deformation). Bone submitted to strain below the yield point can return into its original shape and avoid micro-damage. In the case where strain exerted on bone is above the yield point micro-cracks can occur. The cracks can be repaired but if the mechanical load persists, bone can reach a point of failure and develop stress fractures (Einhorn, 1992; Hart et al., 2017; Turner, 2006). Further studies are needed to investigate the influence of increased dietary P on bone mechanical properties under conditions of increased mechanical load, for example confinement, crowding, and handling stress.

5. Conclusions

The current study identifies several types of vertebral deformities which regress, stabilise, progress, or develop *de novo*, late in seawater. Deformities present in freshwater which affect vertebral centra without affecting the intervertebral joints have the potential to recover in seawater. These deformities include HDV, mild compressions, and vertical shifts. Curiously, HDV in this study are unilateral with ectopic cartilage occupying the bone marrow spaces on the left side of HDV while the right side remains intact. Deformities which affect both, the vertebral centra and the intervertebral joints, do not recover in seawater. These deformities can be grouped into three categories: containment, progression (compressions and progressive vertebral fusion), or late-onset (vertical shift, compressions and fusions). The most severe deformity type observed in the current study was progressive vertebral fusion. Progressive vertebral fusion arise in freshwater, progress, and do not recover in seawater. On the other hand, late-onset vertical shifts, late-onset compressions and fusions, and stable vertebral fusion are less severe. The current findings clearly show the unappreciated potential of several vertebral deformities to recover under favourable conditions whereas deformities of the intervertebral spaces that affect more than three vertebral bodies worsen over time. These results can help fish health personnel to predict the fate of the vertebral deformity development.

Funding

LD and PEW acknowledge funding from the European Union's Horizon 2020 research and innovation programme under the Marie Sklodowska-Curie grant agreement No. 766347 (Biomedaqu) and from Ghent University, Bijzonder Onderzoeksfonds, grant code BOF. ITN.2021.0013.001.

CRediT authorship contribution statement

Lucia Drábiková: Conceptualisation, Data curation, Formal analysis, Investigation, Methodology, Project administration, Software, Visualisation, Writing – original draft, Writing – review & editing. **Per Gunnar Fjelldal:** Investigation, Methodology, Software, Writing – review & editing. **Adelbert De Clercq:** Formal analysis, Writing – review & editing. **M. Naveed Yousaf:** Methodology, Project administration, Writing – review & editing. **Thea Morken:** Methodology, Formal analysis, Investigation, Writing – review & editing. **Charles McGurk:** Project administration, Resources, Writing – review & editing. **P. Eckhard Witten:** Conceptualisation, Project administration, Data curation, Formal analysis, Funding acquisition, Investigation, Methodology, Resources, Supervision, Writing – original draft, Writing – review & editing.

Declaration of Competing Interest

The authors declare that they have no known competing financial interests or personal relationships that could have appeared to influence the work reported in this paper.

Acknowledgements

LD would like to express her gratitude to the whole team at Skretting Aquaculture Innovation Lerang Research Station and especially to Tårn Helgøy Thomsen for running the experiment and helping with the sampling. Also, a thank you to Øyvind Røn and Østby Pederson for help with the analysis and Pedro Borges for help during sample collection. Skretting Aquaculture Innovation Feed Technology Plant (Stavanger, Norway) provided the experimental diets and the rearing facilities for the experiment at Lerang Research Station, Forsand, Norway.

References

Arratia, G., Schultze, H.-P., 1992. Reevaluation of the caudal skeleton of certain actinopterygian fishes: III. Salmonidae. Homologization of caudal skeletal structures. J. Morphol. 214, 187–249. https://doi.org/10.1002/jmor.1052140209.

Arratia, G., Schultze, H.P., Casciotta, J., 2001. Vertebral column and associated elements in dipnoans and comparison with other fishes: development and homology. J. Morphol. 250, 101–172. https://doi.org/10.1002/jmor.1062.

Austreng, E., Storebakken, T., Asgard, T., 1987. Growth rate estimates for cultured Atlantic salmon and rainbow trout. Aquaculture 60, 157–160.

Baeverfjord, G., Hjelde, K., Helland, S., Refstie, S., 2009. The effect of minerals on juvenile Atlantic salmon. In: Baeverfjord, G., Helland, S., Hough, C. (Eds.), Control of Malformations in Fish Aquaculture: Science and Practice. Federation of European Aquaculture Producers. RapidPress, Luxembourgh, pp. 62–66.

Baeverfjord, G., Prabhu, P.A.J., Fjelldal, P.G., Albrektsen, S., Hatlen, B., Lundebye, A., 2019. Mineral nutrition and bone health in salmonids. Rev. Aquac. 11, 740–765. https://doi.org/10.1111/raq.12255.

Bensimon-Brito, A., Cancela, M.L., Huysseune, A., Witten, P.E., 2012. Vestiges, rudiments and fusion events: the zebrafish caudal fin endoskeleton in an evo-devo perspective. Evol. Dev. 14, 116–127. https://doi.org/10.1111/j.1525-142X.2011.00526.x.

Berge, G.M., Witten, P.E., Baeverfjord, G., Vegusdal, A., Wadsworth, S., Ruyter, B., 2009. Diets with different n−6/n−3 fatty acid ratio in diets for juvenile Atlantic salmon, effects on growth, body composition, bone development and eicosanoid production. Aquaculture 296, 299–308. https://doi.org/10.1016/j.aquaculture.2009.08.029.

Björnsson, B.T., Hemre, G.-I., Bjørnevik, M., Hansen, T., 2000. Photoperiod regulation of plasma growth hormone levels during induced smoltification of underyearling Atlantic salmon. Gen. Comp. Endocrinol. 119, 17–25. https://doi.org/10.1006/gcen.2000.7439.

Britz, R., Johnson, G.D., 2005. Occipito-vertebral fusion in ocean sunfishes (Teleostei: Tetraodontiformes: Molidae) and its phylogenetic implications. J. Morphol. 266, 74–79. https://doi.org/10.1002/jmor.10366.

Busacker, G.P., Adelman, I.R., Goolish, E.M., 1990. Growth. In: Schreck, C.B., Moyle, P.B. (Eds.), Methods for Fish Biology. Am. Fish. Soc, Bethesda, pp. 363–387.

Clarkson, M., Taylor, J.F., McStay, E., Palmer, M.J., Clokie, B.G.J., Migaud, H., 2021. A temperature shift during embryogenesis impacts prevalence of deformity in diploid and triploid Atlantic salmon (*Salmo salar* L.). Aquac. Res. 52, 906–923. https://doi.org/10.1111/are.14945.

Clercq, De, Adelbert, Perrott, M.R., Davie, P.S., Preece, M.A., Owen, M.A.G., Witten, P.E., 2018. Temperature sensitive regions of the Chinook salmon vertebral column: vestiges and meristic variation. J. Morphol. 279, 1301–1311. https://doi.org/10.1002/jmor.20871.

De Clercq, A., Perrott, M.R., Davie, P.S., Preece, M.A., Huysseune, A., Witten, P.E., 2017a. The external phenotype–skeleton link in post-hatch farmed Chinook salmon (*Oncorhynchus tshawytscha*). J. Fish Dis. 41, 511–527. https://doi.org/10.1111/jfd.12753.

De Clercq, A., Perrott, M.R., Davie, P.S., Preece, M.A., Wybourne, B., Ruff, N., Witten, P. E., 2017b. Vertebral column regionalisation in Chinook salmon, *Oncorhynchus tshawytscha*. J. Anat. 231, 500–514. https://doi.org/10.1111/joa.12655.

Deschamps, M.-H., Labbé, L., Baloche, S., Fouchereau-Péron, M., Dufour, S., Sire, J.-Y., 2009. Sustained exercise improves vertebral histomorphometry and modulates hormonal levels in rainbow trout. Aquaculture 296, 337–346. https://doi.org/10.1016/j.aquaculture.2009.07.016.

Drábiková, L., Fjelldal, P.G., De Clercq, A., Yousaf, M.N., Morken, T., McGurk, C., Witten, P.E., 2021. Vertebral column adaptations in juvenile Atlantic salmon *Salmo salar*, L. as a response to dietary phosphorus. Aquaculture, 736776. https://doi.org/10.1016/j.aquaculture.2021.736776.

Einhorn, T.A., 1992. Bone strength: the bottom line. Calcif. Tissue Int. 51, 333–339. https://doi.org/10.1007/BF00316875.

Favaloro, E., Mazzola, A., 2000. Meristic character analysis and skeletal anomalies during growth in reared sharpsnout seabream. Aquac. Int. 8, 417–430. https://doi.org/10.1023/A:1009284421354.

Fjelldal, P.G., Grotmol, S., Kryvi, H., Gjerdet, N.R., Taranger, G.L., Hansen, T., Totland, G.K., 2004. Pinealectomy induces malformation of the spine and reduces the mechanical strength of the vertebrae in Atlantic salmon, *Salmo salar*. J. Pineal Res. 36, 132–139. https://doi.org/10.1046/j.1600-079X.2003.00109.x.

Fjelldal, P.G., Lock, E.-J., Grotmol, S., Totland, G.K., Nordgarden, U., Flik, G., Hansen, T., 2006. Impact of smolt production strategy on vertebral growth and mineralisation during smoltification and the early seawater phase in Atlantic salmon (*Salmo salar*, L.). Aquaculture 261, 715–728. https://doi.org/10.1016/j.aquaculture.2006.08.008.

Fjelldal, P.G., Nordgarden, U., Berg, A., Grotmol, S., Totland, G.K., Wargelius, A., Hansen, T., 2005. Vertebrae of the trunk and tail display different growth rates in response to photoperiod in Atlantic salmon *Salmo salar* L., post-smolts. Aquaculture 250, 516–524. https://doi.org/10.1016/j.aquaculture.2005.04.056.

Fjelldal, P.G., Hansen, T.J., Berg, A.E., 2007a. A radiological study on the development of vertebral deformities in cultured Atlantic salmon (*Salmo salar* L.). Aquaculture 273, 721–728. https://doi.org/10.1016/j.aquaculture.2007.07.009.

Fjelldal, P.G., Nordgarden, U., Hansen, T., 2007b. The mineral content affects vertebral morphology in underyearling smolt of Atlantic salmon (*Salmo salar* L.). Aquaculture 270, 231–239. https://doi.org/10.1016/j.aquaculture.2007.03.008.

Fjelldal, P.G., Hansen, T., Breck, O., Sandvik, R., Waagbø, R., Berg, A., Ørnsrud, R., 2009a. Supplementation of dietary minerals during the early seawater phase increase vertebral strength and reduce the prevalence of vertebral deformities in fast-growing under-yearling Atlantic salmon (*Salmo salar* L.) smolt. Aquac. Nutr. 15, 366–378. https://doi.org/10.1111/j.1365-2095.2008.00601.x.

Fjelldal, P.G., van der Meeren, T., Jørstad, K.E., Hansen, T.J., 2009b. A radiological study on vertebral deformities in cultured and wild Atlantic cod (*Gadus morhua*, L.). Aquaculture 289, 6–12. https://doi.org/10.1016/j.aquaculture.2008.12.025.

Fjelldal, P.G., Hansen, T., Breck, O., Ørnsrud, R., Lock, E.J., Waagbø, R., Eckhard Witten, P., 2012. Vertebral deformities in farmed Atlantic salmon (*Salmo salar* L.) - etiology and pathology. J. Appl. Ichthyol. 28, 433–440. https://doi.org/10.1111/j.1439-0426.2012.01980.x.

Fjelldal, P.G., Hansen, T.J., Lock, E.J., Wargelius, A., Fraser, T.W.K., Sambraus, F., Ørnsrud, R., 2016. Increased dietary phosphorous prevents vertebral deformities in triploid Atlantic salmon (*Salmo salar* L.). Aquac. Nutr. 22, 72–90. https://doi.org/10.1111/anu.12238.

Ford, E., 1937. Vertebral variation in teleostean fishes. J. Mar. Biol. Assoc. U. K. 22, 1–60.

Fragkoulis, S., Printzi, A., Geladakis, G., Katribouzas, N., Koumoundouros, G., 2019. Recovery of haemal lordosis in gilthead seabream (*Sparus aurata* L.). Sci. Rep. 9, 9832. https://doi.org/10.1038/s41598-019-46334-1.

Fragkoulis, S., Kourkouta, C., Geladakis, G., Printzi, A., Glaropoulos, A., Koumoundouros, G., 2022. Recovery of Haemal Lordosis in European Seabass *Dicentrarchus labrax* (Linnaeus 1758). Aquac. J. https://doi.org/10.3390/aquacj2010001.

Fraser, T.W.K., Witten, P.E., Albrektsen, S., Breck, O., Fontanillas, R., Nankervis, L., Fjelldal, P.G., 2019. Phosphorus nutrition in farmed Atlantic salmon (*Salmo salar*): life stage and temperature effects on bone pathologies. Aquaculture 511. https://doi.org/10.1016/j.aquaculture.2019.734246.

Gil Martens, L., Witten, P.E., Fivelstad, S., Huysseune, A., Sævareid, B., Vikeså, V., Obach, A., 2006. Impact of high water carbon dioxide levels on Atlantic salmon smolts (*Salmo salar* L.): effects on fish performance, vertebrae composition and structure. Aquaculture 261, 80–88. https://doi.org/10.1016/j.aquaculture.2006.06.031.

Gil Martens, L., Fjelldal, P.G., Lock, E.-J., Wargelius, A., Wergeland, H., Witten, P.E., Ørnsrud, R., 2012. Dietary phosphorus does not reduce the risk for spinal deformities in a model of adjuvant-induced inflammation in Atlantic salmon (*Salmo salar*) postsmolts. Aquac. Nutr. 18, 12–20. https://doi.org/10.1111/j.1365-2095.2011.00871.x.

Gill, C.D., Fisk, D.M., 1966. Vertebral abnormalities in Sockeye, Pink and Chum Salmon. Trans. Am. Fish. Soc. 95, 177–182. https://doi.org/10.1577/1548-8659(1966)95.

Grini, A., Hansen, T., Berg, A., Wargelius, A., Fjelldal, P.G., 2011. The effect of water temperature on vertebral deformities and vaccine-induced abdominal lesions in Atlantic salmon, *Salmo salar* L. J. Fish Dis. 34, 531–546. https://doi.org/10.1111/j.1365-2761.2011.01265.x.

Hall, B.K., Witten, P.E., 2019. Plasticity and variation of skeletal cells and tissues and the evolutionary development of actinopterygian fishes. In: Johanson, Z.,

Underwood, C., Richter, M. (Eds.), Evolution and Development of Fishes. Cambridge University Press, Cambridge, pp. 126–143.
Hamilton, S.J., Mehrle, P.M., Mayer, F.L., Jones, J.R., 1981. Method to evaluate mechanical properties of bone in fish. Trans. Am. Fish. Soc. 110, 708–717. https://doi.org/10.1577/1548-8659(1981)110<708:MTEMPO>2.0.CO;2.
Handeland, S.O., Wilkinson, E., Sveinsbø, B., McCormick, S.D., Stefansson, S.O., 2004. Temperature influence on the development and loss of seawater tolerance in two fast-growing strains of Atlantic salmon. Aquaculture 233, 513–529. https://doi.org/10.1016/j.aquaculture.2003.08.028.
Hansen, T., Fjelldal, P.G., Yurtseva, A., Berg, A., 2010. A possible relation between growth and number of deformed vertebrae in Atlantic salmon (*Salmo salar* L.). J. Appl. Ichthyol. 26, 355–359. https://doi.org/10.1111/j.1439-0426.2010.01434.x.
Hart, N.H., Nimphius, S., Rantalainen, T., Ireland, A., Siafarikas, A., Newton, R.U., 2017. Mechanical basis of bone strength: influence of bone material, bone structure and muscle action. J. Musculoskelet. Neuronal Interact. 17, 114–139.
Helland, S., Refstie, S., Espmark, Å., Hjelde, K., Baeverfjord, G., 2005. Mineral balance and bone formation in fast-growing Atlantic salmon parr (*Salmo salar*) in response to dissolved metabolic carbon dioxide and restricted dietary phosphorus supply. Aquaculture 250, 364–376. https://doi.org/10.1016/j.aquaculture.2005.03.032.
Helland, S., Denstadli, V., Witten, P.E., Hjelde, K., Storebakken, T., Skrede, A., Baeverfjord, G., 2006. Hyper dense vertebrae and mineral content in Atlantic salmon (*Salmo salar* L.) fed diets with graded levels of phytic acid. Aquaculture 261, 603–614. https://doi.org/10.1016/j.aquaculture.2006.08.027.
Holm, H., Ytteborg, E., Høst, V., Reed, A.K., Dalum, A.S., Bæverfjord, G., 2020. A pathomorphological description of cross-stitch vertebrae in farmed Atlantic salmon (*Salmo salar* L.). Aquaculture 526, 735382. https://doi.org/10.1016/j.aquaculture.2020.735382.
Johanson, Z., Sutija, M., Joss, J., 2005. Regionalization of axial skeleton in the lungfish *Neoceratodus forsteri* (Dipnoi). J. Exp. Zool. Part B Mol. Dev. Evol. 304B, 229–237. https://doi.org/10.1002/jez.b.21048.
Kranenbarg, S., 2005. Adaptive bone formation in acellular vertebrae of sea bass (*Dicentrarchus labrax* L.). J. Exp. Biol. 208, 3493–3502. https://doi.org/10.1242/jeb.01808.
Kranenbarg, S., Waarsing, J.H., Muller, M., Weinans, H., van Leeuwen, J.L., 2005. Lordotic vertebrae in sea bass (*Dicentrarchus labrax* L.) are adapted to increased loads. J. Biomech. 38, 1239–1246. https://doi.org/10.1016/j.jbiomech.2004.06.011.
Kvellestad, A., Høie, S., Thorud, K., Tørud, B., Lyngøy, A., 2000. Platyspondyly and shortness of vertebral column in farmed Atlantic salmon *Salmo salar* in Norway-description and interpretation of pathologic changes. Dis. Aquat. Org. 39, 97–108. https://doi.org/10.3354/dao039097.
Lall, S., 2022. The minerals. In: Hardy, R.W., Kaushik, S.J. (Eds.), Fish Nutrition, 4th edition. Academic press, Inc., San Diego, pp. 469–554. https://doi.org/10.1016/B978-0-12-819587-1.00005-7.
Lall, S.P., Lewis-McCrea, L.M., 2007. Role of nutrients in skeletal metabolism and pathology in fish - an overview. Aquaculture 267, 3–19. https://doi.org/10.1016/j.aquaculture.2007.02.053.
Lovett, B.A., Firth, E.C., Tuck, I.D., Symonds, J.E., Walker, S.P., Perrott, M.R., Herbert, N. A., 2020. Radiographic characterisation of spinal curvature development in farmed New Zealand Chinook salmon *Oncorhynchus tshawytscha* throughout seawater production. Sci. Rep. 10, 20039. https://doi.org/10.1038/s41598-020-77121-y.
Madaro, A., Kjøglum, S., Hansen, T., Fjelldal, P.G., Stien, L.H., 2021. A comparison of triploid and diploid Atlantic salmon (*Salmo salar*) performance and welfare under commercial farming conditions in Norway. J. Appl. Aquac. 1–15 https://doi.org/10.1080/10454438.2021.1916671.
Munday, J.S., Perrott, M.R., Symonds, J.E., Walker, S.P., Lovett, B., Preece, M.A., Davie, P.S., 2016. Unilateral perivertebral fibrosis associated with lordosis, kyphosis and scoliosis (LKS) in farmed Chinook salmon in New Zealand. Dis. Aquat. Org. 121, 211–221. https://doi.org/10.3354/dao03056.
NRC, 2011. Nutrient Requirements of Fish and Shrimp. The National Academic Press, Washinghton D.C.
Pauwels, F., 1960. Eine neue theorie über den einfluß mechanischer reize auf die differenzierung der stützgewebe. Z. Anat. Entwicklungsgesch. 121, 478–515. https://doi.org/10.1007/BF00523401.
Perrott, M., Symonds, J., Walker, S., Hely, F., Wybourne, B., Preece, M., Davie, P., 2018. Spinal curvatures and onset of vertebral deformities in farmed Chinook salmon, *Oncorhynchus tshawytscha* (Walbaum, 1792) in New Zealand. J. Appl. Ichthyol. 34 https://doi.org/10.1111/jai.13663.
Presnell, J.K., Schreibman, M.P., 1998. Humason's Animal Tissue Techniques, 5th ed. The John Hopkins University Press, Baltimore.
Printzi, A., Fragkoulis, S., Dimitriadi, A., Keklikoglou, K., Arvanitidis, C., Witten, P.E., Koumoundouros, G., 2021. Exercise-induced lordosis in zebrafish *Danio rerio* (Hamilton, 1822). J. Fish Biol. 98, 987–994. https://doi.org/10.1111/jfb.14240.
Sambraus, B.F., Glover, K.A., Hansen, T., Fraser, T.W.K., Solberg, M.F., Fjelldal, P.G., 2014. Vertebra Deformities in Wild Atlantic Salmon Caught in the Figgjo River, Southwest, 30, pp. 777–782. https://doi.org/10.1111/jai.12517.
Sambraus, F., Hansen, T., Daae, B.S., Thorsen, A., Sandvik, R., Stien, L.H., Fjelldal, P.G., 2020. Triploid Atlantic salmon *Salmo salar* have a higher dietary phosphorus requirement for bone mineralisation during early development. J. Fish Biol. 1–11 https://doi.org/10.1111/jfb.14338.
Sánchez, R.C., Obregón, E.B., Rauco, M.R., 2011. Hypoxia is like an ethiological factor in vertebral column deformity of salmon (*Salmo salar*). Aquaculture 316, 13–19. https://doi.org/10.1016/j.aquaculture.2011.03.012.
Sfakiotakis, M., Lane, D., Davies, J., 1999. Review of fish swimming modes for aquatic locomotion. Ocean. Eng. IEEE J. 24, 237–252. https://doi.org/10.1109/48.757275.
Smedley, M.A., Migaud, H., McStay, E.L., Clarkson, M., Bozzolla, P., Campbell, P., Taylor, J.F., 2018. Impact of dietary phosphorous in diploid and triploid Atlantic salmon (*Salmo salar* L.) with reference to early skeletal development in freshwater. Aquaculture 490, 329–343. https://doi.org/10.1016/j.aquaculture.2018.02.049.
Solstorm, F., Solstorm, D., Oppedal, F., Gunnar, P., 2016. The Vertebral Column and Exercise in Atlantic Salmon — Regional Effects, 461, pp. 9–16. https://doi.org/10.1016/j.aquaculture.2016.04.019.
Sullivan, M., Hammond, G., Roberts, R.J., Manchester, N.J., 2007. Spinal deformation in commercially cultured Atlantic salmon, *Salmo salar* L.: a clinical and radiological study. J. Fish Dis. 30, 745–752. https://doi.org/10.1111/j.1365-2761.2007.00889.x.
Totland, G.K., Fjelldal, P.G., Kryvi, H., Løkka, G., Wargelius, A., Sagstad, A., Grotmol, S., 2011. Sustained swimming increases the mineral content and osteocyte density of salmon vertebral bone. J. Anat. 219, 490–501. https://doi.org/10.1111/j.1469-7580.2011.01399.x.
Trangerud, C., Bjørgen, H., Koppang, E.O., Grøntvedt, R.N., Skogmo, H.K., Ottesen, N., Kvellestad, A., 2020. Vertebral column deformity with curved cross-stitch vertebrae in Norwegian seawater-farmed Atlantic salmon, *Salmo salar* L. J. Fish Dis. 43, 379–389. https://doi.org/10.1111/jfd.13136.
Turner, C.H., 2006. Bone strength: current concepts. Ann. N. Y. Acad. Sci. 1068, 429–446. https://doi.org/10.1196/annals.1346.039.
Vågsholm, I., Djupvik, H.O., 1998. Risk factors for spinal deformities in Atlantic salmon, *Salmo salar* L. J. Fish Dis. 21, 47–53. https://doi.org/10.1046/j.1365-2761.1998.00069.x.
Vera, L.M., Lock, E.-J., Hamre, K., Migaud, H., Leeming, D., Tocher, D.R., Taylor, J.F., 2019. Enhanced micronutrient supplementation in low marine diets reduced vertebral malformation in diploid and triploid Atlantic salmon (*Salmo salar*) parr, and increased vertebral expression of bone biomarker genes in diploids. Comp. Biochem. Physiol. Part B Biochem. Mol. Biol. 237, 110327 https://doi.org/10.1016/j.cbpb.2019.110327.
Wargelius, A., Fjelldal, P.G., Hansen, T., 2005. Heat shock during early somitogenesis induces caudal vertebral column defects in Atlantic salmon (*Salmo salar*). Dev. Genes Evol. 215, 350–357. https://doi.org/10.1007/s00427-005-0482-0.
Weinans, H., Prendergast, P.J., 1996. Tissue adaptation as a dynamical process far from equilibrium. Bone 19, 143–149. https://doi.org/10.1016/8756-3282(96)00143-3.
Witten, P.E., Huysseune, A., 2009. A comparative view on mechanisms and functions of skeletal remodelling in teleost fish, with special emphasis on osteoclasts and their function. Biol. Rev. 84, 315–346. https://doi.org/10.1111/j.1469-185X.2009.00077.x.
Witten, P.E., Hansen, A., Hall, B.K., 2001. Features of Mono- and Multinucleated Bone Resorbing Cells of the Zebrafish *Danio rerio* and Their Contribution to Skeletal Development, Remodeling, and Growth, 207, pp. 197–207.
Witten, P.E., Gil Martens, L., Hall, B.K., Huysseune, A., Obach, A., 2005. Compressed vertebrae in Atlantic salmon *Salmo salar*: evidence for metaplastic chondrogenesis as a skeletogenic response late in ontogeny. Dis. Aquat. Org. 64, 237–246. https://doi.org/10.3354/dao064237.
Witten, P.E., Obach, A., Huysseune, A., Baeverfjord, G., 2006. Vertebrae fusion in Atlantic salmon (*Salmo salar*): development, aggravation and pathways of containment. Aquaculture 258, 164–172. https://doi.org/10.1016/j.aquaculture.2006.05.005.
Witten, P.E., Gil-Martens, L., Huysseune, A., Takle, H., Hjelde, K., 2009. Towards a classification and an understanding of developmental relationships of vertebral body malformations in Atlantic salmon (*Salmo salar* L.). Aquaculture 295, 6–14. https://doi.org/10.1016/j.aquaculture.2009.06.037.
Witten, P.E., Owen, M.A.G., Fontanillas, R., Soenens, M., McGurk, C., Obach, A., 2016. A primary phosphorus-deficient skeletal phenotype in juvenile Atlantic salmon *Salmo salar*: the uncoupling of bone formation and mineralization. J. Fish Biol. 88, 690–708.
Witten, P.E., Fjelldal, P.G., Huysseune, A., McGurk, C., Obach, A., Owen, M.A.G., 2019. Bone without minerals and its secondary mineralization in Atlantic salmon (*Salmo salar*): the recovery from phosphorus deficiency. J. Exp. Biol. https://doi.org/10.1242/jeb.188763 jeb.188763.
Ytteborg, E., Baeverfjord, G., Torgersen, J., Hjelde, K., Takle, H., 2010a. Molecular pathology of vertebral deformities in hyperthermic Atlantic salmon (*Salmo Salar*). BMC Physiol. 10 https://doi.org/10.1186/1472-6793-10-12.
Ytteborg, E., Torgersen, J.S., Pedersen, M.E., Baeverfjord, G., Hannesson, K.O., Takle, H., 2010b. Remodeling of the notochord during development of vertebral fusions in Atlantic salmon (*Salmo salar*). Cell Tissue Res. 342, 363–376. https://doi.org/10.1007/s00441-010-1069-2.
Ytteborg, E., Baeverfjord, G., Lock, E.J., Pedersen, M., Takle, H., Ørnsrud, R., Albrektsen, S., 2016. Utilization of acid hydrolysed phosphorous from herring bone by-products in feed for Atlantic salmon (*Salmo salar*) start-feeding fry. Aquaculture 459, 173–184. https://doi.org/10.1016/j.aquaculture.2016.03.031.